Lidar assisted wake redirection in wind farms: A data driven approach

Dhiman, H. S., Deb, D., & Foley, A. M. (2020). Lidar assisted wake redirection in wind farms: A data driven approach. *Renewable Energy*, *152*, 484-493. https://doi.org/10.1016/j.renene.2020.01.027

Published in:
Renewable Energy

Document Version:
Peer reviewed version

Elsevier Editorial System(tm) for Renewable Energy

Manuscript Draft

Manuscript Number: RENE-D-19-02722R1

Title: Lidar assisted wake redirection in wind farms: A data driven approach

Article Type: Research Paper

Keywords: Center of Wake; Lidar; Transfer function; Velocity deficit; Yaw angle; Wake effect

Corresponding Author: Professor Dipankar Deb, PhD

Corresponding Author's Institution: Institute of Infrastructure Technology Research and Management

First Author: Harsh S Dhiman, M. Tech

Order of Authors: Harsh S Dhiman, M. Tech; Dipankar Deb; Aoife Foley, PhD

Abstract: Lidar based wind measurement is an integral part of wind farm control. The major issues and challenges in power maximization include the potential losses due to wake effect observed among wind turbines. This manuscript presents a wake management technique that utilizes lidar simulations for wake redirection. The proposed methodology is validated for 2-turbine and 15-turbine wind farm layouts involving a PI control based yaw angle correction. Yaw angle misalignment using wake center tracking of the upstream turbines is used to increase the power generation levels. Results of wake center estimation are compared with a Kalman filter based method. Further, the velocity deficit and overall farm power improvement by yaw angle correction is calculated. Results reveal a 1.7% and 0.675% increase in total wind farm power for two different wind speed cases.

***Title Page**

Title:
Lidar assisted wake redirection in wind farms: A data driven approach

Harsh S. Dhiman
Department of Electrical Engineering,
Institute of Infrastructure Technology Research and Management,
Ahmedabad, India 380026.
Email: harsh.dhiman.17pe@iitram.ac.in

Dipankar Deb (Corresponding author)*
Department of Electrical Engineering,
Institute of Infrastructure Technology Research and Management,
Ahmedabad, India 380026.
Email: dipankardeb@iitram.ac.in

Aoife M. Foley
School of Mechanical and Aerospace Engineering,
Queen's University,
Belfast, Northern Ireland, United Kingdom BT9 5AH
Email: a.foley@qub.ac.uk

***Cover Letter**

From:
Dr. Dipankar Deb
Department of Electrical Engineering,
Institute of Infrastructure Technology Research and Management,
Ahmedabad, Gujarat, India- 380026.
October 23, 2019

To,
Editor-in-chief,
Renewable Energy.

Dear Dr. Soteris Kalogirou,

We would like to submit this revised manuscript by Harsh S. Dhiman, Dr. Dipankar Deb and Dr. Aoife M. Foley entitled "Lidar assisted wake redirection in wind farms: A data driven approach" to Renewable Energy for possible publication. This paper highlights the wake management in wind farms by accurately controlling the wake center for increased power output in different wake scenarios. It may be of interest to the readers of your journal.

We have meticulously gone through each and every comment from the reviewers. The comments from the reviewers have been addressed thoroughly and are highlighted in blue text in the revised manuscript. We thank the reviewers for their comments that has helped to improve the manuscript quality.
We confirm that there is no conflict of interest and affirm that this manuscript is original, has not been published before and is not currently being considered for publication in other journal.

Thank you very much for your attention to our paper.

Correspondence related to the paper may please be directed to Dr. Dipankar Deb, at the following address, telephone and fax number, and e-mail address:

Dr. Dipankar Deb
Department of Electrical Engineering
Institute of Infrastructure Technology Research and Management
Ahmedabad, Gujarat, India 380026
Tel: - (+91)-7203954452
Email: - dipankardeb@iitram.ac.in

Sincerely yours,
Dr. Dipankar Deb

Response to Reviewer #1

The comments are addressed in blue highlighted text in the revised manuscript.

Reviewer #1: The paper RENE-D-19-02722 paper proposes a wake management technique based on transfer function methodology obtained after lidar simulations for wake redirection. The proposed methodology is validated for 2-turbine and 15-turbine wind farm layouts involving a PI control based yaw angle correction. Yaw angle misalignment based on tracking wake center of the upstream turbines is used to increase the power generation levels. Results of wake center estimation are compared with a Kalman filter based method.

Further, the velocity deficit and total wind farm power improvement by yaw angle correction is calculated. Results reveal a 1.7% increase in total wind farm power.

In my opinion, the submitted manuscript is very good written, it has a clear aim and the potential reader understand the target of the scientific effort. There is define and robust methodology and well-presented scientific clear analysis based on real data and certain conclusions.

From the scientific point of view authors give clearly the followed methodology and an analytical scientific review has done.

Also, the manuscript under evaluation needs some corrections because is not so clear the extract of 1.7% of increase in power. Moreover the validation is probably only for 15 wind turbines windfarm, with wind speed range of 8-10m/s. So, it will more acceptable if there is study for speeds from 4 to 25 m/s.

In addition, at figure 7 the windfarm power is W? Which the nominal capacity of the windfarm. Please change the word power, to capacity.

Recapitulating, and taking into consideration the above-mentioned indicative comments, I believe that the quality of this paper is acceptable and clear to the final reader, but needs minor revision so it can be accepted for publication in the Renewable Energy Journal.

- ***Response: We thank the reviewer for the comment. The power improvement study for 15-turbine wind farm layout for wind speed range 4-25 m/sec is present in lines 272-287 on page 16-17, Section 5 of the revised manuscript. The power improvement for each wind turbine in the yawed mode is tabulated in Table 2 on Page 18 of the revised manuscript.***
- ***We have also changed the y-axis label of Figure 7 to "Farm Capacity".***

Once again we thank the reviewer for appreciating our work.

Response to Reviewer #2

The comments are addressed in blue highlighted text in the revised manuscript.

GENERAL COMMENTS: The paper is well written and some minor changes should be considered for the final version. The paper presents an interesting study with useful results that are accurately framed into the literature. The manuscript merits publication. I would like to congratulate the authors on the clear and easy to follow manuscript, with almost no typos or errors.

The paper is recommended for publication as it presents an interesting contribution for wind turbines' planning and windfarms' design, towards a more efficient infrastructure. I wonder how this study could be extended to offshore structures, in which not only the wind flow affects the power generation of the turbines, but the wave-current flow and the turbines alignment or misalignment can influence the natural frequency of each foundation, including the severity of scour phenomena for example. Maybe these ideas could be looked into as a future works developed by this team.

ABSTRACT

Seems well-written and straight the point, nothing to add here.

HIGHLIGHTS

Nothing to add here

1 - INTRODUCTION

Line 30: "models, which" (comma missing)

- ***Response: We thank the reviewer for the comment. The comma is now inserted at the appropriate place in line 25 on page 2 of the revised manuscript.***

Line 32-33: what is the acceptable range? Please specify.

- ***Response: We thank the reviewer for raising the concern with the range. The range of the wake losses is in between 10-20%. The same is now corrected in lines 27-28 on page 2 of the revised manuscript.***

Line 49: first time an abbreviation appears please put it in the format "extended form (abbreviation)".

- ***Response: We thank the reviewer for the comment. The abbreviation is now put into its correct form as suggested. The same is updated in line 45 on page 3 of the revised manuscript.***

Line 59: the same as in 49 for PI. Correct this aspect throughout the paper

- ***Response: We thank the reviewer for the comment. The abbreviation for PI is corrected in line 51 on page 3 of the revised manuscript.***

Line 85: "wind farms, which" (comma missing)

- ***Response: We thank the reviewer for the comment. The missing comma is now put into its required place in line 57 on page 3 of the revised manuscript.***

Line 138: Kalmer instead of kalmer

- ***Response: We thank the reviewer for the comment. The punctuation error is corrected in line 94 on page 5 of the revised manuscript.***

Comment: The introduction is well-written and the authors made an effort to raise works and summarize them in terms of the results and highlight the important aspects for the remaining sections of the paper. However, the intro is way too lengthy and definitely needs be cut down, maybe into 2/3 or half of its current size.

- ***Response: We thank the reviewer for the comment. We have reduced the introduction and made it more appropriate for the readers.***

2 - Multi-model Wake center estimation and control of Wind Farms

Equation 1: the letter D formerly designates the rotor diameter. I think a different symbol should be used for the damping factor here, or in the rotor case, to avoid redundancy of the nomenclature.

- ***Response: We thank the reviewer for the comment. Symbol for damping factor is changed to ζ in line 121 on page 6 of the revised manuscript.***

Line 167: missing a comma again before the word which the same has been corrected before, please correct this throughout the paper when appropriate.

- ***Response: We thank the reviewer for the comment. The missing comma is now inserted at its appropriate place in line 123 on page 6 of the revised manuscript.***

Equation 5: now the rotor diameter has the symbol D0 please make sure your symbols are consistent in the manuscript.

- ***Response: We thank the reviewer for the comment. The Symbol for rotor diameter is updated as D_0 throughout the manuscript.***

line 177: The model parameter kd is selected as 0.15 - ok, but why? the value came out of the blue.

- ***Response: We thank the reviewer for the comment. The parameter k_d is a model parameter that defines wake recovery. For a neutral atmospheric boundary layer it is taken as 0.15 and a suitable reference is cited in lines 134-135 on page 7 of the revised manuscript.***

Equation 9: CT has already appeared before, please definite it in the Equation 6

- ***Response: We thank the reviewer for the comment. The symbol C_T is defined in line 130-131 on page 6 of the revised manuscript.***

Line 291-220: The empirical relationship between effective wake center and effective velocity deficit has been estimated using curve fitting toolbox in MATLAB. - How was it fitted? Regression? more details should be given here, or else other authors will find it very difficult to reproduce your work and results…this type of sentences does not benefit the paper, as it may give the appearance that Matlab was used as a "black-box" where little to no knowledge is needed for its application. As it seems, by the way the previous sections are written that this is not the case, thus I recommend the authors to provide more information every now and then when the Matlab software (or similar) is referred to. The same is valid for example in line 223 for the SIT package…

- ***Response: We thank the reviewer for the comment. The details about the curve fitting toolbox and system identification toolbox are provided in lines 177-182 on page 10 and lines 195-200 on page 11 of the revised manuscript.***

Comment: The section is well-written and there are no major comments here, sometimes the authors just make a ref to Matlab packages etc, which could be eventually avoided or at least minimised.

3 - Performance parameters for waked wind farms

Nothing to add here.

4 - Numerical Simulations for Proposed Methodology Line 278: avoid the use of personal pronouns such as "we"…please use a more formal language. correct this in this and next sections.

- ***Response: We thank the reviewer for the comment. The language is now more formal and the corrections are made at suitable places such as line 244 on page 13 of the revised manuscript.***

Nothing much to add.

5 - Discussion

As in some parts of section 4, but definitely in section 5, I enjoyed the authors effort in making sure their results were framed into the previously made studies. This made it easy to ensure that the results can be understood in terms of their contribution to the topic.

We thank the reviewer for appreciating the work.

Highlights

- Lidar assisted wake control is studied.
- Transfer function-based methodology for wake center control is proposed.
- Wake center control for multiple wind turbines is presented.
- Methodology is validated for two wind speed scenarios for a 15-turbine farm layout.
- Power improvement in non-yawed and yawed mode is studied.

Lidar assisted wake redirection in wind farms: A data driven approach

Harsh S. Dhiman[a], Dipankar Deb[a], Aoife M. Foley[b]

[a] *Department of Electrical Engineering, Institute of Infrastructure Technology Research and Management, Ahmedabad, India 380026.*

[b] *School of Mechanical and Aerospace Engineering, Queens University, Belfast, Northern Ireland, United Kingdom BT9 5AH*

Abstract

Lidar based wind measurement is an integral part of wind farm control. The major issues and challenges in power maximization include the potential losses due to wake effect observed among wind turbines. This manuscript presents a wake management technique that utilizes lidar simulations for wake redirection. The proposed methodology is validated for 2-turbine and 15-turbine wind farm layouts involving a PI control based yaw angle correction. Yaw angle misalignment using wake center tracking of the upstream turbines is used to increase the power generation levels. Results of wake center estimation are compared with a Kalman filter based method. Further, the velocity deficit and overall farm power improvement by yaw angle correction is calculated. Results reveal a 1.7% and 0.675% increase in total wind farm power for two different wind speed cases.

Keywords: Center of Wake, Lidar, Transfer function, Velocity deficit, Yaw angle, Wake effect

Abbreviations

HAWT Horizontal Axis Wind Turbine

Email addresses: harsh.dhiman.17pe@iitram.ac.in (Harsh S. Dhiman), dipankardeb@iitram.ac.in (Dipankar Deb), a.foley@qub.ac.uk (Aoife M. Foley)

IPC	Individual Pitch Control
LIDAR	Light Detection and Ranging
PI	Proportional Integral Control

1. Introduction

Growing energy demands are rapidly facilitating the wind turbine installations globally in the form of large wind parks to convert the energy available from moving air to electrical energy. Due to constrained land area and cost of equipment one has to design a proper wind farm layout for energy generation [1]. Wind power capture by wind turbine is affected by many factors like wind direction, speed and optimal turbine spacing [2]. For a given terrain, wind turbines must be placed at an optimal operating distance from each other to avoid potential derating caused by wind wakes which are aerodynamic phenomena leading to (a) reduction in wind speed magnitude at the downstream turbine, and (b) increased air turbulence causing mechanical loading on the turbine structure [3]. Sethi et al. presented the modelling of wind farms considering wake interactions [4]. The wake effect is studied in terms of effective wind speed for wind farm layouts. Wind wakes typically are dominant over near wake and far wake region that extend up to $4D_0$ and $8D_0$ respectively, where D_0 is the rotor diameter. Wind wakes causing power loss for an individual wind turbine, has led to the development of many analytical and field models to study the same [5].

Among analytical models, Jensen's [6], Frandsen's [7] and Ainslie's [8] wake model form kinematic wake models, which commonly use algebraic equations to characterize wake deficit. Jensen's wake model is validated and tested for accommodating the power losses due to wake effect and are found in an acceptable range of 10-20% [9, 10, 11, 12]. A new two dimensional Jensen wake model is proposed by Tian et al. that incorporates a variable wake decay rate rather than a constant one. Numerical simulations are performed for computing the wake deficit and are compared with field measurements. Results reveal that such a wake model underestimates for near-wake regions [13]. Ishihara et al. have presented an analytical model that encapsulates the effect of thrust coefficient and air turbulence on the wake deficit [14]. The numerical simulations are compared with a test carried out in wind tunnel and results of the proposed analytical model are in good agreement with experimental analysis. In terms of Large-eddy simulation (LES), the wake flow is studied in neutral atmospheric boundary layer, where the aerodynamic effects on the rotor body and blade element are modeled separately in order to assess power losses [15, 16, 17].

Experimental results from a wind turbine with rotor diameter 0.9 m placed 4 rotor diameters from the wind inlet section and wake velocity distribution, and measured at a downstream distance of $0.6D_0$ and $3D_0$ have shown up to 40% power loss and 80% increased dynamic loading on the turbine structure [18]. Wake study is also important in Wind farm layout optimization (WFLOP) where optimal placement of the wind turbines leads to to minimum wake effect and maximum power capture [19]. Gonzalez et al. have further discussed an evolution based algorithm for optimal wind farm layout [20] to determine net power produced considering the losses occurred due to wake effects. Pitch and yaw angle control techniques are two common ways of increasing power capture. Schlipf et al. demonstrated a Proportional-Integral (PI) control based pitch controller that mitigates dynamic load variations in rotor speed caused due to severe conditions up to 80% [21]. The performance of a traditional feedback control is tested against feed-forward blade pitch control to achieve dynamic load mitigation along with improved life. Results reveal that the feed-forward controller performs better [22].

Vali et al. have utilized a MPAC method for wind farms, to minimize the reference error in wind farm [23]. A methodology based on adjoint MPC is implemented for 6-turbine wind farm where the time-varying signal is tracked against a reference power. Experimental analysis for power improvement using yaw control is studied in [24] for longitudinal distances of $3D_0$ and $6D_0$. In terms of power optimization, a yaw angle based approach is adopted, for single column wind farm layout where axial induction factor for downstream turbines is kept fixed [25]. An experimental study for a small-scale turbine with wake structure and turbine parameters such as yaw angle, pitch angle and tip speed ratio are monitored for a favorable operating performance [26]. In [27], Lidar assisted measurements along with a look-ahead controller is adopted to curb dynamic load through fatigue analysis. A concept of an equivalent load generated given the load is subjected to exact load for its entire lifetime is utilized. In [28], for generator speed regulation, a wind-scheduled control is analysed where for the conditions above rated value, Lidar based control suppresses the irregularities in an accurate wind speed measurement. In [29], Lidar is leveraged to trace the flow caused due wake effect and a desired yaw angle set point is achieved.

In a wind farm where the power losses are incurred due to wake, velocity deficit can be used as a standardized parameter to characterize losses. Given the spatial coordinates (a, b, c) representing the position in the wake field representing maximum power loss, the region is termed as the wake center. Cacciola et al. have used the hub loads and sensors at the downwind turbine to acquire wind velocity deficit data and horizontal shear via an optimization approach for wake center detection without considering yaw misalignment [30]. In [31], authors have discussed an autonomous wake characterization approach to identify wake center position for nonidentical atmospheric conditions. A Doppler lidar is used to scan from January 2017 to June 2017 and results indicate that the wake center position shifts when stable atmospheric conditions exist. Raach et al. explored the possibility of implementing a H_∞ controller for wake redirection based on yaw angle control and a closed-loop performance for the system is analysed [32]. In [33], a wake management strategy is presented using adaptive control technique for wind farms where uncertainties are dominant. Further in [34], decision making and control aspect for a hybrid wind farm are discussed.

The prime contribution of this manuscript is LIDAR based simulation for closed-loop wake center control. The wind turbine and wake are modeled as transfer functions and the estimated wake center is made to follow a desired reference yaw angle trajectory. The proposed methodology is validated for a 15 turbine wind farm layout and the power improvement for each turbine is assessed when upstream turbine(s) are yawed. The wake center estimation are compared with Kalman filter estimations. The subsequent sections are organized as follows. Section 2 entails wake center estimation for multi-model and multiple wake scenario based on proposed transfer function based methodology and Kalman filter. Section 3 highlights performance parameters like farm power production and air turbulence whereas Section 4 discusses the simulation results for proposed methodology and Kalman filter method for a 15-turbine farm configuration. Section 5 highlights discussions, and is followed by Conclusions.

2. Multi-model Wake center estimation and control of Wind Farms

Closed-loop control methodology, as applied to wind farms, primarily built around two main tasks: (i) measures the estimated wind field and, (ii) controls the wake center position. Wind field measurement using lidar accurately processes the controller requirements. LIDAR (Light Detection and Ranging System) sensor utilizes laser based detection and ranging to measure an upstream turbine's effective wind speed at d_{lidar}, the lidar distance. The yaw angle modification potentially reduces the power delivered by an upstream turbine and causes the reverse effect on the downstream turbine. The calculation of the wind speed is done prior to the interaction of the incident wind with the turbine, so as to provide sufficient time for real-time control action [35]. Subsystems related to closed-loop control based on PI control of wake center estimation are described next for desired yaw angle, in Figure 1.

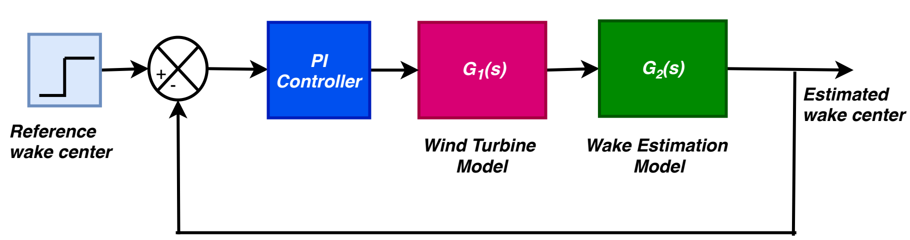

Figure 1: Block diagram for the system under study

2.1. Wind turbine model and wake center estimation

Using actuator disk theory, the power delivered from i^{th} turbine is given as

$$P_i = \frac{1}{2}\rho A_0 C_p u_i^3, \tag{1}$$

for density of air ρ, swept area A_0, power coefficient C_p, and wind speed u_i for i^{th} turbine [36]. However, for wind turbines in yawed condition, the output obtained from an upstream turbine is modified by $\cos^q \gamma$, with q being a tunable parameter in the range $(1.4, 2.2)$ as reported by Fleming et al. [37]. The yaw dynamics for an upstream turbine is expressed as

$$\ddot{\gamma} + 2\zeta\omega\dot{\gamma} = \omega^2 \left(\gamma_{ref} - \gamma\right), \tag{2}$$

for undamped eigen frequency ω, damping factor ζ, desired yaw angle γ_{ref}.

The transfer function is estimated with an accuracy of 99.99% using system identification toolbox with γ_{ref} as input and γ as the actual yaw angle, which is varied from (-25°, 25°), with $n_p = 2$ poles and $n_z = 1$ zero, determined as

$$G_1(s) = \frac{0.533s + 0.01094}{s^2 + 0.1538s + 0.002736}. \tag{3}$$

Optimized output in yawed condition of a turbine as formulated by Qian et al. [38] is expressed as

$$P_i = \frac{1}{2}\rho A_0 C_p u_i^3 \cos^2(\gamma_i). \tag{4}$$

The deflection in wake flow caused due to yaw position for a given upstream turbine, as postulated by Jimnez et al. [39], is

$$\delta(d) = \frac{\xi_{init}\Big(15\big(\frac{2k_d d}{D_0}+1\big)^4 + \xi_{init}^2\Big)}{\frac{30k_d}{D_0}\big(\frac{2k_d d}{D_0}+1\big)^5} - \frac{\xi_{init} D_0 (15 + \xi_{init}^2)}{30k_d}, \tag{5}$$

$$\xi_{init}(\gamma, C_T) = \frac{1}{2}\cos^2(\gamma)\sin(\gamma) C_T, \tag{6}$$

where ξ_{init} is the initial wake angle, d is the scanning or preview distance used by lidar, D_0 is the rotor diameter, k_d is the uncertain model parameter and C_T is the thrust coefficient.

For computation of wake center deflection with changing yaw angles, appropriate lidar distance d_{lidar} is chosen for accurate calculation of the transfer function [40]. A suitable value of the model parameter k_d is selected as 0.15 owing to the turbine operation in neutral boundary layer [41]. The transfer function with 93.76% accuracy for $n_p = 2$ poles and $n_z = 0$ zeros, is of the form

$$G_2(s) = \frac{-0.158}{s^2 + 2.56 \times 10^{-12}s + 0.2404}. \quad (7)$$

The wake center needs to be controlled to ultimately maximize the wind farm power generated. A simple PI controller is tuned using tuning feature of MATLAB/Simulink, is described as

$$f = K_p\Big(\delta(\gamma) + \frac{1}{T_i}\int \delta(\gamma)dt\Big), \quad (8)$$

where $\delta(\gamma)$ is the estimated wake center, K_p, T_i are the proportional gain and time constant.

2.2. Multi-model Wake center control

The accuracy of the estimation of wake center relies on aspects such as ξ_{init}, d, rotor diameter (D_0) and k_d as in (5). Multi-model wake center estimation is studied with constant k_d, and the scanning distance, d_{lidar} is modified in multiples of D_0. Table 1 highlights the estimation accuracies of the transfer function models. Using system identification toolbox and different lidar scanning distances, the best fit models are obtained.

Table 1: Estimation accuracies for different lidar scanning distances

Scanning distance, d_{lidar}	Estimation Accuracy (%)
$1D_0$	93.76
$1.5D_0$	95.08
$2D_0$	94.94
$2.5D_0$	94.82
$3D_0$	94.71

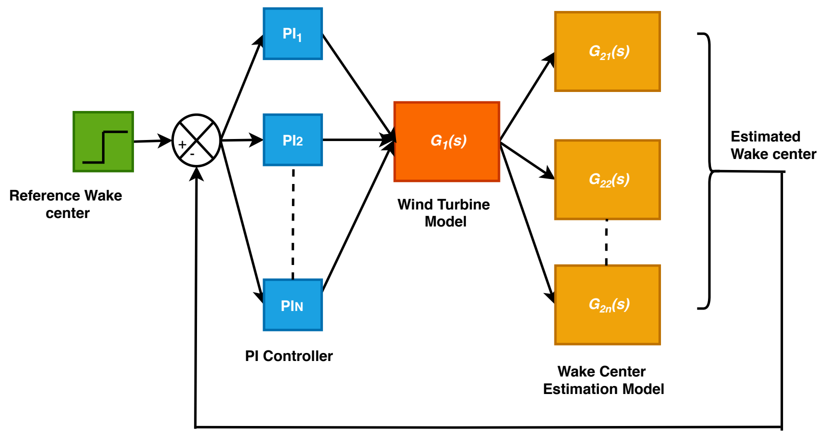

Figure 2: Multi-model wake center estimation

Figure 2 illustrates wake center estimation for a multi-model scenario. Bastankhah and Porte-Agel [42] describe a wake model which follows a Gaussian profile for wind speed deficit. Mathematically, it is expressed as a function of thrust coefficient C_T, radial distance r, and wake width x.

$$v = v_0\Big(1 - A(x)e^{\frac{-r^2}{2\sigma^2}}\Big), \tag{9}$$

$$A(x) = 1 - \sqrt{1 - \frac{C_T}{8(\sigma/D_0)^2}}, \tag{10}$$

$$\frac{\sigma}{D_0} = k\frac{x}{D_0} + \epsilon, \tag{11}$$

where $A(x)$ denotes the maximum normalized velocity deficit for a distance x, and wake width σ which is a function of k representing wake entrainment constant. According to linear superposition principle, the wake deficit due to upstream turbine(s) is expressed as

$$\Delta v_i = \sum_{j=1}^{N}\Big(1 - \frac{v_j}{v_0}\Big), \tag{12}$$

for j^{th} upstream turbine, overall velocity deficit Δu_i at i^{th} downstream turbine, and total upstream turbines N. In [43], a quadratic superposition is presented and is expressed as

$$\Delta v_i = \sqrt{\sum_{j=1}^{N}(\Delta v_j)^2}. \tag{13}$$

In non-yawed conditions, power generated at the downstream turbine dwindles because of shadow effect of upstream turbines, and requires effective wake management. Yawing the upstream turbine effectively controls the wake center, and to account for multiple wakes on a downstream turbine from a multiple of upstream turbines, the transformed thrust coefficient $C_T \cos^3(\gamma_{w,j})$, where $\gamma_{w,j}$ denotes the yaw angle for the j^{th} upwind turbine. Further, modified velocity deficit for i^{th} downstream turbine is expressed as

$$v_i = v_0\Big(1 - A_{ij}(x)e^{\frac{-r^2}{2\sigma_{ij}^2}}\Big), \tag{14}$$

$$A_{ij}(x) = 1 - \sqrt{1 - \frac{C_T \cos^3(\gamma_{w,j})}{8(\sigma_{ij}/D_0)^2}}, \tag{15}$$

$$\frac{\sigma_{ij}}{D_0} = k\frac{x_{ij}}{D_0} + \epsilon, \tag{16}$$

$$\beta_w = 0.5\left(\frac{1 + \sqrt{1 - C_T}}{\sqrt{1 - C_T}}\right), \tag{17}$$

where $\epsilon = 0.25\sqrt{\beta_w}$, σ_{ij} represents wake width at downstream distance x_{ij} between j^{th} upstream and i^{th} downstream turbine. The velocity deficit for each upstream turbine is computed using (14) for yaw angle $\gamma_{w,j}$ and for N upstream turbines, the overall velocity deficit at i^{th} downstream turbine is calculated based on the principle of quadratic superposition in (13). Figure 3 illustrates the proposed methodology for wake redirection for multiple upstream turbines.

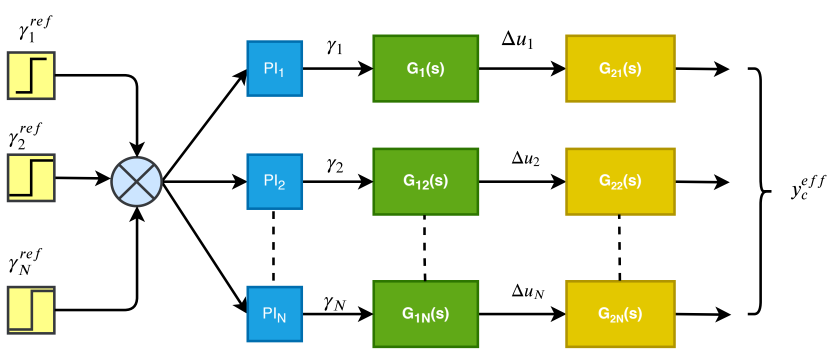

Figure 3: Multiple wake scenario based wake center estimation

Transfer function models with Multiple-Input Single Output (MISO) configuration are evaluated for best estimation accuracy, and is expressed as

$$g(y_c) = v_m e^{\frac{-(y_c-\mu_y)^2}{2\sigma_{lidar}^2}}, \quad (18)$$

$$\sigma_{lidar} = k d_{lidar} + \epsilon D_0, \quad (19)$$

where y_c, μ_y represent the height of hub and position of the wake center respectively given an overall velocity deficit of $g(y_c)$ for a lidar scanning distance d_{lidar} and v_m denotes the maximum velocity deficit. The empirical relationship between effective velocity deficit and effective wake center is estimated using curve fitting toolbox in MATLAB [44]. In the curve fitting toolbox, the input quantity is considered as velocity deficit and output quantity as effective wake center deflection. Using these quantities the curve fitting toolbox utilized for appropriate fitting.

Developed in 1960, Kalman filter is being actively used to estimate the states in the noisy or disturbed environments. State estimation as perceived by a Kalman filter is based on a recursive process of a noisy data [45], and is expressed mathematically as

$$\hat{x}_{t+1} = \mathbf{A}x_t + \mathbf{B}u_t + w_t, \quad (20)$$

$$\hat{y}_t = \mathbf{C}x_t + \mathbf{D}u_t + v_t, \quad (21)$$

where $\mathbf{A}, \mathbf{B}, \mathbf{C}, \mathbf{D}$ represent the state-space matrices of the plant, w_t, v_t are process and measurement noise at time step t respectively and $\hat{x}_{t+1}$ is the updated state vector at time step $t+1$. For the current scenario, Kalman filter technique is implemented to derive an estimate of the wake center trajectory for a set of upwind and downwind turbines. Using system identification toolbox, the transfer function models are computed with yaw angle as input and wake center deflection as output. In Figure 4, a schematic representation for Kalman filter based wake center is illustrated.

The state-space model can be estimated using system identification toolbox available in MATLAB [46]. In this toolbox, the input and output data are fed with a 'double' variable which represents a time-varying quantity. The model simulations can be run for different system orders in order to obtain maximum

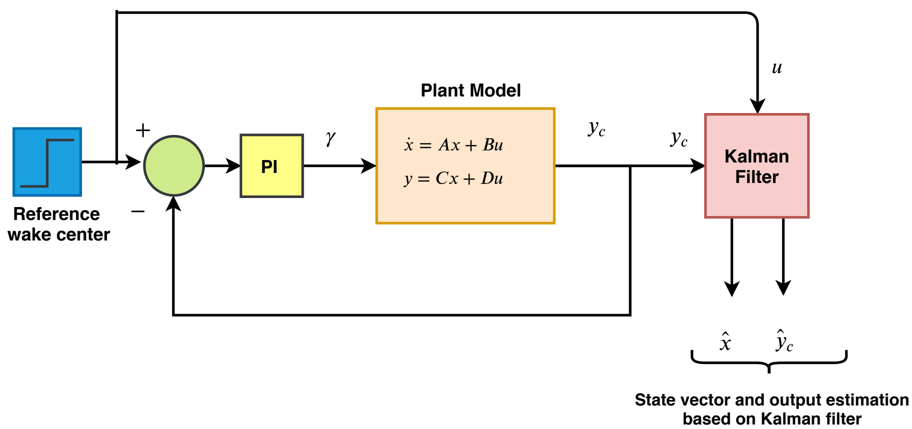

Figure 4: Kalman filter technique based wake center estimation

estimation accuracy. From here, the state-space model can be exported and can be used according to the user need.

3. Performance parameters for waked wind farms

Power maximization and optimization of the land available are the two prime objectives for wind farm operators. In case of wake effect, the reduction in power capture is compensated by either changing yaw alignment or changing lateral position of downstream turbine. Since micro-siting is done in priori, yaw misalignment is the preferred choice. Power capture and air turbulence are the two main parameters that affect the performance of a wind farm. Jensen's wake model computes wind speed at distance h and a distance r radially from the wake center line is expressed as

$$v(h,r) = v_0\Big[1 - 2a\Big(\frac{r_0}{r_0 + kh}\Big)^2\Big], \tag{22}$$

where v_0 is the freestream wind velocity, r_0 denotes rotor radius and k represents wake entrainment factor. The flow behind upwind turbine is deflected by Ω_j when yaw angle is aligned at $\gamma_{w,j}$ and wind direction θ_j expressed as

$$\Omega_j = (0.6a_j + 1)\gamma_{w,j} + \theta_j, \tag{23}$$

where a_j is the axial induction factor for turbine $j \in H$ (upstream turbines). Velocity profile for a downwind turbine with yaw misalignment is given as

$$v_i(x,r) = \begin{cases} v_0\Big[1 - 2a_j\Big(\dfrac{1}{1+2kT\cos(\Omega_j)}\Big)^2 \times \cos^2(4.5\Omega_j)\Big], & \Omega_j \leq 20^\circ \\ v_0, & \Omega_j > 20^\circ, \end{cases} \tag{24}$$

where $T = \frac{h}{D_0} \in [2, \ldots, 5]$ denotes the spacing factor which is a multiple of rotor diameter. A yaw angle of $\gamma_{w,j}$ on the upstream turbine WT_j diverts the wake flow for a downwind turbine WT_i by an angle of Ω_j arrives at a velocity profile like (24). A yawed upstream turbine now captures power which is changed by a factor of $\cos^3 \gamma_w$.

Further, dynamic loading on downstream is a challenging issue that causes catastrophic damage to rotor blades and tower. The resulting air turbulence can be reduced by changing yaw angle $\gamma_{w,j}$ of upstream turbine. Mathematically, the overall turbulence intensity is given as

$$E_{eff} = \sqrt{E_a^2 + K^2 \sum_{j=1}^{N} (1 - \sqrt{1 - C_T \cos\gamma_{w,j}}) h_i^{-2/3}}, \tag{25}$$

where E_a denotes the ambient air turbulence whereas E_{eff} being computed for a downwind distance h_i for N upstream turbines and K is constant with a value of 0.93 [47].

4. Numerical Simulations for Proposed Methodology

Next, the proposed methodology for closed-loop control of wake center for 2-turbine and 15-turbine wind farm layout is presented. For 2-turbine wind farm, the intent is to track wake center of WT_1 (upwind) and examine the impact on the performance parameters of WT_2 (downstream).

Throughout the simulation, wind turbines with same rotor diameter of 80 meters are considered. WT_1 and WT_2 are placed 400 meters apart. The wake center is estimated using lidar simulation for desired yaw control based on methodology discussed in Section 2. Initially, the yaw angle of WT_1 is $\gamma_w = 0^\circ$

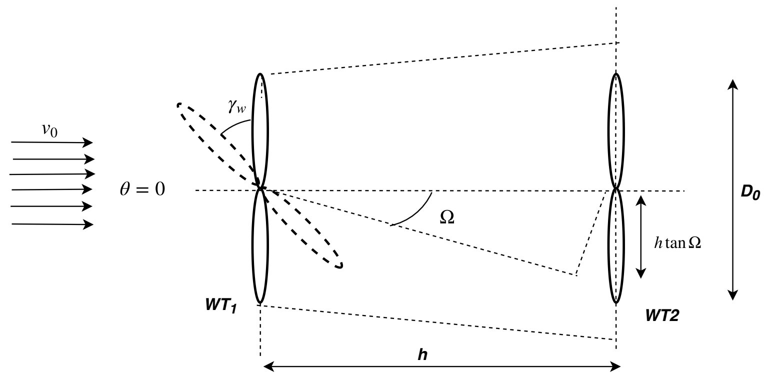

Figure 5: 2-turbine layout for wake deflection

and lidar scanning distance is kept $1D_0$. In order to validate the proposed methodology, a 500 second simulation is carried out for 2-turbine layout. Figure 6 illustrates the wake center simulation using proposed methodology.

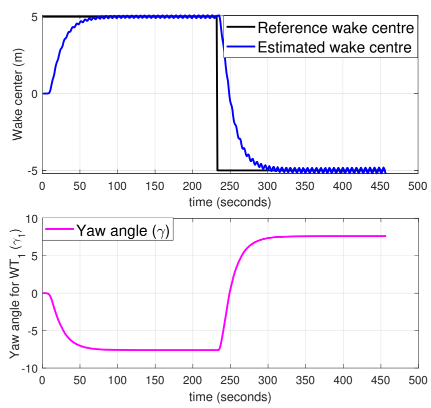

Figure 6: Desired yaw angle alignment and wake center for 2-turbine layout

The wake center reference is changed at t=250 seconds for desired yaw angle setting based on a PI control technique. Based on this, a 1000 second simulation is carried out to evaluate the performance parameters for 2-turbine wind farm layout. The yaw angle setting for WT_1, γ_w is changed at t=500 second where the mean wind speed is changed from 8 m/sec to 10 m/sec.

From Figure 7, it is observed that the total wind power extracted has increased by 7.52%. In a similar study presented by Raach et al. [29] with same rotor diameter of turbines, the total power increase is reported around 4.5%.

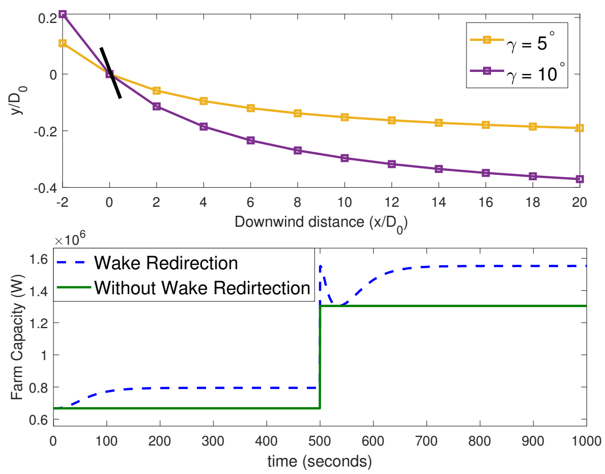

Figure 7: Wake deflection and power output with and without redirection

The net wind farm power increases due to high fidelity lidar measurements that accurately measure the deflection caused by yaw misalignment. The yaw angle misalignment also affects the air turbulence intensity on downstream wind turbine. For a fixed yaw angle of an upstream turbine, the turbulence decreases as the longitudinal distance between the turbines is increased. Figure 8 illustrates the turbulence acting on WT_2 as a result of varying downstream distance.

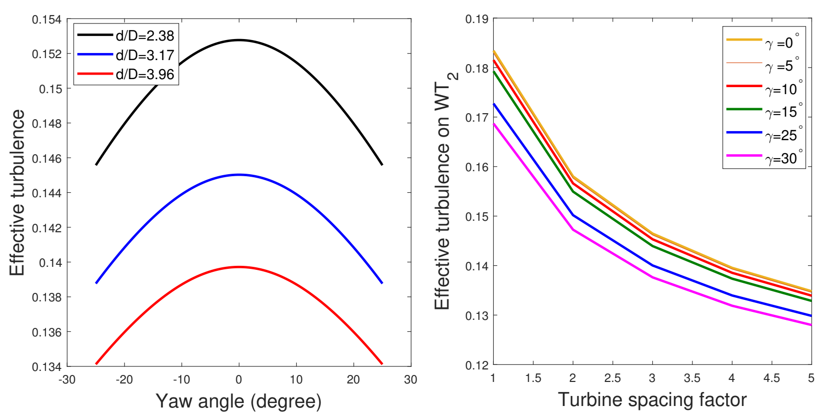

Figure 8: Effective air turbulence at WT_2

Keeping longitudinal distance fixed, for given yaw misalignment, the effective turbulence acting on WT_2 is found minimum for $\gamma_w = 30°$. Wake center control is analyzed for a 15 turbine wind farm with WT_{12} facing wake effect from $WT_2, WT_3, WT_4, WT_5, WT_7, WT_9$ and WT_{10}. In Figure 9, the distances between turbines in terms of rotor diameter are illustrated. Yaw angles of upstream turbines WT_j for $j \in [2, 3, 4, 5, 7, 9, 10]$ are chosen as $\gamma_2 = 2°$, $\gamma_3 = 2.5°$, $\gamma_4 = 5°$, $\gamma_5 = 7°$, $\gamma_7 = 9°$, $\gamma_9 = 10°$ and $\gamma_{10} = 15°$ and when yawed, the wake center deflection is controlled by determining effective velocity deficit.

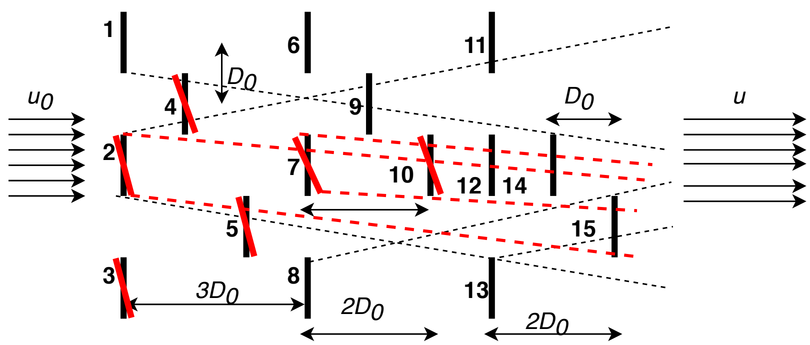

Figure 9: 15 turbine layout in non-yawed (black solid line) and yawed mode(red solid line)

The empirical relationship between overall velocity deficit and wake center deflection (18) is converted into an overall transfer function having multiple-inputs and single output (MISO) topology. LIDAR is mounted at nacelle of WT_{12} that scans the wind flow for all upwind turbines. For estimating the wake width, a scan distance $d_{lidar} = 2D_0$ is considered.

In Figures 10 and 11, the wake center estimation by the proposed transfer function methodology and by Kalman filter based technique is presented.

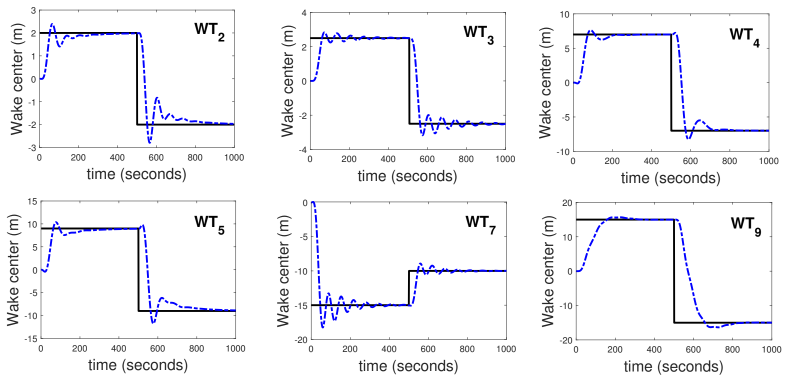

Figure 10: Wake center estimation by proposed model (blue dotted line) and reference wake center (black solid line) for upwind turbines of WT_{12}

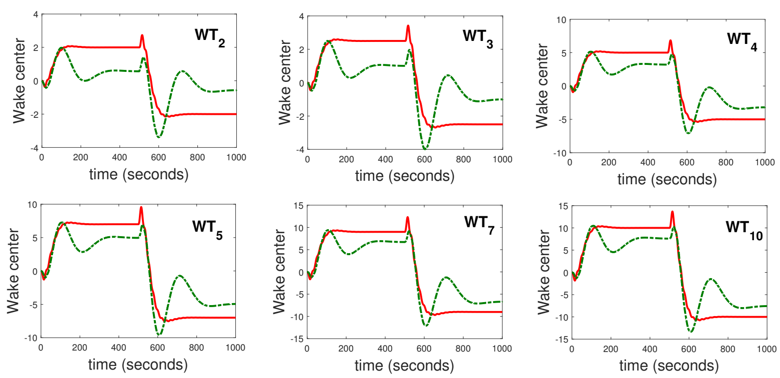

Figure 11: Wake center estimation by proposed model (red solid line) and Kalman filter (green dotted line) for upwind turbines of WT_{12}

5. Discussions

The wind turbine power improvement in the 15-turbine farm layout when operated in yaw mode is tested for a wind profile of 500 seconds illustrated in Figure 12.

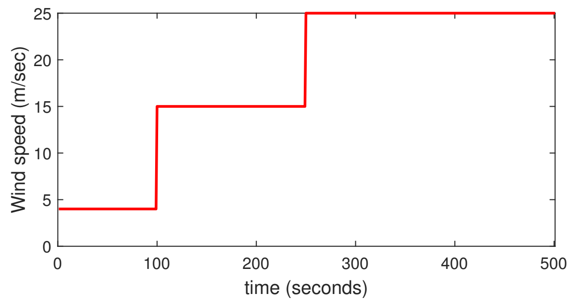

Figure 12: Wind speed profile for the range 4-25 m/sec

The wind in this case ranges from 4 m/sec to 25 m/sec. For the first 100 seconds the wind speed us 4 m/sec, the from 100 to 250 seconds wind speed is 15 m/sec and for the last 250 seconds the speed is 25 m/sec. The mean wind power captured by each wind turbine is calculated for non-yawed (P_{ny}) and yawed (P_y) scenario. Table 2 depicts the improvement in wind power captured for each turbine and it is observed that for WT_1 the wind power captured remains same as it is not yawed. For WT_2 and WT_3, the wind power decreases in yawed mode as they are the upstream turbines. For turbines WT_4 to WT_{15}, the power captured in yawed mode increases as yawing deflects the wake away from downstream turbine. Overall, for the wind speed profile illustrated in Figure 12, the mean power captured by the wind farm in non-yawed mode is 160.3364 MW while in yawed mode it is 161.418 MW thus indicating an increase of 0.675%.

Table 2: Mean turbine power in non-yawed and yawed condition for wind profile in the range 4-25 m/sec

Turbine	Upwind Turbine	Power (P_{ny}) (MW)	Power (P_y) (MW)	% change
WT_1	NA	14.3044	14.3044	0.00
WT_2	NA	14.3044	14.2782	-0.183
WT_3	NA	14.3044	14.2636	-0.285
WT_4	1,2	10.9830	10.9890	+0.0546
WT_5	2,3	11.704	11.709	+0.0427
WT_6	1,4	12.215	12.219	+0.0327
WT_7	2,4,5	9.4873	9.4918	+0.047
WT_8	3,5	10.0182	10.188	+1.690
WT_9	1,4,6,7	9.2660	9.2704	+0.0475
WT_{10}	2,5,7,9	9.2478	9.2519	+0.0440
WT_{11}	1,2,4,6,9	8.9314	9.09320	+1.811
WT_{12}	2,3,4,5,7,9,10	8.9126	9.09261	+1.2734
WT_{13}	3,5,8	8.8956	9.0942	+2.2320
WT_{14}	2,3,4,5,7,9,10,12	8.8831	9.0988	+2.3130
WT_{15}	2,5,7,8,10,12,13,14	8.8792	9.0987	+2.3511
		$\sum P_{ny} = 160.3364$	$\sum P_y = 161.418$	

Table 3: Wind turbine power captured for non-yawed and yawed scenario with wind speed range 8-10 m/sec

Turbine	Upwind Turbine	Power (P_{ny}) (MW)	Power (P_y) (MW)	% change
WT_1	NA	2.8274	2.8274	0.00
WT_2	NA	2.8274	2.8223	-0.1800
WT_3	NA	2.8274	2.8223	-0.1800
WT_4	1,2	1.5074	1.5116	+0.2786
WT_5	2,3	2.6816	2.6916	+0.3729
WT_6	1,4	2.0666	2.0891	+1.0887
WT_7	2,4,5	2.0561	2.1541	+4.7663
WT_8	3,5	2.0162	2.1130	+4.8011
WT_9	1,4,6,7	2.0053	2.1016	+4.8022
WT_{10}	2,5,7,9	2.0001	2.0884	+4.4414
WT_{11}	1,2,4,6,9	2.0761	2.0962	+0.9681
WT_{12}	2,3,4,5,7,9,10	1.9821	1.9959	+0.6962
WT_{13}	3,5,8	2.0752	2.0965	+0.9782
WT_{14}	2,3,4,5,7,9,10,12	1.9701	1.9862	+0.8172
WT_{15}	2,5,7,8,10,12,13,14	1.9970	2.0866	+4.4867
		$\sum P_{ny} = 32.916$	$\sum P_y = 33.483$	

Results from Figures 10 and 11 indicate that Kalman filter based technique fails to track the wake center deflection accurately due to nonlinear nature and stochastic of wind speed. Contrary to Kalman filter, the proposed transfer function based technique tracks the reference wake center with accuracy. The velocity deficit caused due to each upwind turbine for this layout is computed both in yawed and non-yawed conditions using the Gaussian wake profile (13). In Figure 13, the overall velocity deficit in yawed mode the deficit is 6.15% less than that in non-yawed mode.

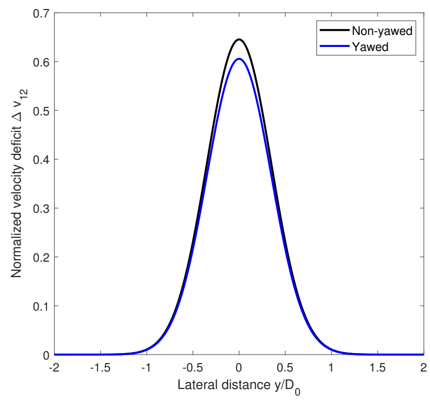

Figure 13: Non-yawed and yawed scenarios for overall velocity deficit

Further, Figure 14 illustrates the normalized velocity at WT_{12} for different upwind turbines.

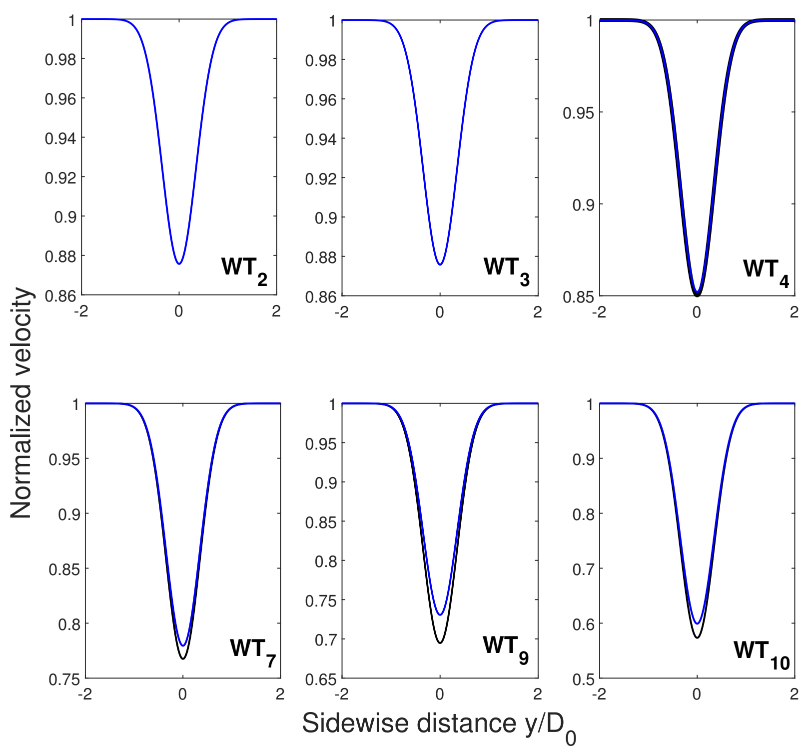

Figure 14: Normalized velocity for WT_{12} for non-yawed (black) and yawed (blue) scenario

Velocity for WT_2 and WT_3 renders the fact that the due to the large longitudinal distance ($6D_0$) to WT_{12}, the velocity deficit with yaw misaligned is not pronounced. Further, for WT_7, WT_9 and WT_{10} power capture is found to be notable when the upwind turbines are yawed. At $y/D_0 = 0$, the turbine power is minimum as it indicates the wake center position. Table 3 highlights the wind power tapped by respective turbines with reference to the layout shown in Figure 9. The powers for non-yawed (P_{ny}) and yawed (P_y) scenario are calculated with a freestream wind speed of $v_0 = 10$ m/sec, and the power capture with yawed upwind turbines outperforms that in non-yawed scenario for each turbine. A 1.7% rise in the overall farm power is observed with operation in the yawed scenario. In other related analyses for power maximization with yaw correction, Adaramola et al. carried a wind tunnel experiment to study the outcome of yawing the upwind turbine on the downwind turbine [24] and observed a noteworthy increase in the power coefficient of downstream turbine at $3D_0$ downstream distance away. Since the proposed methodology is solely based on the transfer function blocks, the computational complexity for analyzing the wind farm performance does not arise. Dynamic scenarios in the atmospheric boundary layer pose significant challenges to wake center estimation in form of turbulent eddies that arise due to Coriolis forces. With availability of accurate wind measurement devices like Lidar, wind farm controllers can take appropriate actions to cope with time periods of power sags. Further, experimental investigation carried out by General Electric suggests that managing turbulent wakes increases the plant energy output in the range of 0.5-2% [48].

6. Conclusions and Future scope

A novel closed loop control methodology aimed at effective tracking of the wake center of the upwind turbine, that is based on transfer function formulation is proposed in the present work. Taking leverage of a data drive approach, a transfer function model relating yaw angle and wake center for a multiple wake case is estimated. To determine the effective wake center for a given upwind turbine WT_{12}, the overall velocity deficit as seen by WT_{12} is used. Utilizing advanced controllers, wake management integrates scenarios that deal with stochastic wind environment along with micro-siting related issues. In the present case, lidar based measurement methodology outperforms Kalman filter technique in a more accurate wake center estimation. Scenarios with different wind conditions in the range of 8-10 m/sec and 4-25 m/sec are tested and results indicate an increase of 1.7% and 0.675% respectively. This study can be extended in future for offshore wind platform where the dominant wave-current will have a significant influence on the dynamic loading of the turbine structure.

Acknowledgements

Dr Foley's research is funded by the Northern Ireland Department for Economics, the Engineering and Physical Sciences Research Council (EPSRC) and NSFC jointly funded iGIVE project (EP/L001063/1), the Collaborative REsearch of Decentralization, ElectrificatioN, Communications and Economics (CREDENCE) project, which is funded by a US-Ireland Department for the Economy (DfE), Science Foundation Ireland (SFI), National Science Foundation (NSF) and Research and Development Partnership Program (Centre to Centre) award (grant number USI 110) and the SPIRE2 (Storage Platform for the Integration of Renewable Energy 2) project, funded by the Special European Programmes Body (SEUPB) under the European Unions INTERREG VA programme.

References

[1] S. Chowdhury, J. Zhang, A. Messac, L. Castillo, Unrestricted wind farm layout optimization (UWFLO): Investigating key factors influencing the maximum power generation, Renewable Energy 38 (1) (2012) 16–30.

[2] J. F. Manwell, Wind energy explained : theory, design and application, Wiley, Chichester, U.K, 2009.

[3] C. L. Archer, A. Vasel-Be-Hagh, C. Yan, S. Wu, Y. Pan, J. F. Brodie, A. E. Maguire, Review and evaluation of wake loss models for wind energy applications, Applied Energy 226 (2018) 1187–1207.

[4] J. K. Sethi, D. Deb, M. Malakar, Modeling of a wind turbine farm in presence of wake interactions, in: 2011 International Conference on Energy, Automation and Signal, IEEE, 2011.

[5] T. Göçmen, P. van der Laan, P.-E. Réthoré, A. P. Diaz, G. C. Larsen, S. Ott, Wind turbine wake models developed at the technical university of denmark: A review, Renewable and Sustainable Energy Reviews 60 (2016) 752–769.

[6] N. Jensen, A note on wind generator interaction, 1983.

[7] S. Frandsen, R. Barthelmie, S. Pryor, O. Rathmann, S. Larsen, J. Højstrup, M. Thøgersen, Analytical modelling of wind speed deficit in large offshore wind farms, Wind Energy 9 (1-2) (2006) 39–53.

[8] J. Ainslie, Calculating the flowfield in the wake of wind turbines, Journal of Wind Engineering and Industrial Aerodynamics 27 (1-3) (1988) 213–224.

[9] A. Crespo, J. Hernndez, S. Frandsen, Survey of modelling methods for wind turbine wakes and wind farms, Wind Energy 2 (1) (1999) 1–24.

[10] R. J. Barthelmie, K. Hansen, S. T. Frandsen, O. Rathmann, J. G. Schepers, W. Schlez, J. Phillips, K. Rados, A. Zervos, E. S. Politis, P. K. Chaviaropoulos, Modelling and measuring flow and wind turbine wakes in large wind farms offshore, Wind Energy 12 (5) (2009) 431–444.

[11] F. Porté-Agel, Y.-T. Wu, C.-H. Chen, A numerical study of the effects of wind direction on turbine wakes and power losses in a large wind farm, Energies 6 (10) (2013) 5297–5313.

[12] Y.-K. Wu, Y.-S. Su, Z. Lee, T.-Y. Wu, Estimation of wake losses in an offshore wind farm by WAsP - a real project case study in taiwan, in: 10th

International Conference on Advances in Power System Control, Operation & Management (APSCOM 2015), Institution of Engineering and Technology, 2015. doi:10.1049/ic.2015.0264.

[13] L. Tian, W. Zhu, W. Shen, N. Zhao, Z. Shen, Development and validation of a new two-dimensional wake model for wind turbine wakes, Journal of Wind Engineering and Industrial Aerodynamics 137 (2015) 90–99.

[14] T. Ishihara, G.-W. Qian, A new gaussian-based analytical wake model for wind turbines considering ambient turbulence intensities and thrust coefficient effects, Journal of Wind Engineering and Industrial Aerodynamics 177 (2018) 275–292.

[15] R. J. Stevens, L. A. Martínez-Tossas, C. Meneveau, Comparison of wind farm large eddy simulations using actuator disk and actuator line models with wind tunnel experiments, Renewable Energy 116 (2018) 470–478.

[16] F. Porté-Agel, Y.-T. Wu, H. Lu, R. J. Conzemius, Large-eddy simulation of atmospheric boundary layer flow through wind turbines and wind farms, Journal of Wind Engineering and Industrial Aerodynamics 99 (4) (2011) 154–168.

[17] Y.-T. Wu, F. Porté-Agel, Modeling turbine wakes and power losses within a wind farm using LES: An application to the horns rev offshore wind farm, Renewable Energy 75 (2015) 945–955.

[18] H. Schümann, F. Pierella, L. Sætran, Experimental investigation of wind turbine wakes in the wind tunnel, Energy Procedia 35 (2013) 285–296.

[19] J. Park, K. H. Law, Layout optimization for maximizing wind farm power production using sequential convex programming, Applied Energy 151 (2015) 320–334.

[20] J. S. González, A. G. G. Rodriguez, J. C. Mora, J. R. Santos, M. B. Payan, Optimization of wind farm turbines layout using an evolutive algorithm, Renewable Energy 35 (8) (2010) 1671–1681.

[21] D. Schlipf, M. Kühn, Prospects of a collective pitch control by means of predictive disturbance compensation assisted by wind speed measurements, Proceedings of the 9th German Wind Energy Conference DEWEK, 26th to 27th November, Bremen, Germany, 2008.

[22] F. Dunne, L. Pao, A. Wright, B. Jonkman, N. Kelley, Combining standard feedback controllers with feedforward blade pitch control for load mitigation in wind turbines, in: 48th AIAA Aerospace Sciences Meeting Including the New Horizons Forum and Aerospace Exposition, American Institute of Aeronautics and Astronautics, 2010.

[23] M. Vali, V. Petrovic, S. Boersma, J.-W. van Wingerden, L. Y. Pao, M. Kuhn, Model predictive active power control of waked wind farms, in: 2018 Annual American Control Conference (ACC), IEEE, 2018.

[24] M. Adaramola, P.-Å. Krogstad, Experimental investigation of wake effects on wind turbine performance, Renewable Energy 36 (8) (2011) 2078–2086.

[25] Z. Dar, K. Kar, O. Sahni, J. H. Chow, Windfarm power optimization using yaw angle control, IEEE Transactions on Sustainable Energy 8 (1) (2017) 104–116.

[26] B. Dou, M. Guala, L. Lei, P. Zeng, Experimental investigation of the performance and wake effect of a small-scale wind turbine in a wind tunnel, Energy 166 (2019) 819–833.

[27] D. Schlipf, T. Fischer, C. E. Carcangiu, M. Rossetti, E. Bossanyi, Load analysis of look-ahead collective pitch control using lidar, Proceedings of the 10th German Wind Energy Conference DEWEK, 2010.

[28] V. Rezaei, LIDAR-based robust wind-scheduled control of wind turbines, in: 2014 American Control Conference, IEEE, 2014.

[29] S. Raach, D. Schlipf, P. W. Cheng, Lidar-based wake tracking for closed-loop wind farm control, Journal of Physics: Conference Series 753 (2016) 052009.

[30] S. Cacciola, M. Bertelè, J. Schreiber, C. Bottasso, Wake center position tracking using downstream wind turbine hub loads, Journal of Physics: Conference Series 753 (2016) 032036.

[31] R. J. Barthelmie, S. C. Pryor, Automated wind turbine wake characterization in complex terrain, Atmospheric Measurement Techniques Discussions (2019) 1–31.

[32] S. Raach, D. Schlipf, F. Borisade, P. W. Cheng, Wake redirecting using feedback control to improve the power output of wind farms, in: 2016 American Control Conference (ACC), IEEE, 2016.

[33] H. S. Dhiman, D. Deb, V. Muresan, V. E. Balas, Wake management in wind farms: An adaptive control approach, Energies 12 (7). doi:10.3390/en12071247.

[34] H. S. Dhiman, D. Deb, Decision and Control in Hybrid Wind Farms, Springer Singapore, 2020. doi:10.1007/978-981-15-0275-0.

[35] E. Simley, L. Pao, R. Frehlich, B. Jonkman, N. Kelley, Analysis of wind speed measurements using continuous wave LIDAR for wind turbine control, in: 49th AIAA Aerospace Sciences Meeting including the New Horizons Forum and Aerospace Exposition, American Institute of Aeronautics and Astronautics, 2011.

[36] The wind and wind turbines, in: Wind Turbine Control Systems, Springer London, 2007, pp. 7–28.

[37] P. Fleming, J. Annoni, J. J. Shah, L. Wang, S. Ananthan, Z. Zhang, K. Hutchings, P. Wang, W. Chen, L. Chen, Field test of wake steering at an offshore wind farm, Wind Energy Science 2 (1) (2017) 229–239.

[38] G.-W. Qian, T. Ishihara, A new analytical wake model for yawed wind turbines, Energies 11 (3) (2018) 665.

[39] Á. Jiménez, A. Crespo, E. Migoya, Application of a LES technique to characterize the wake deflection of a wind turbine in yaw, Wind Energy 13 (6) (2009) 559–572.

[40] E. Machefaux, G. C. Larsen, N. Troldborg, M. Gaunaa, A. Rettenmeier, Empirical modeling of single-wake advection and expansion using full-scale pulsed lidar-based measurements, Wind Energy 18 (12) (2014) 2085–2103.

[41] L. Vollmer, G. Steinfeld, D. Heinemann, M. Kühn, Estimating the wake deflection downstream of a wind turbine in different atmospheric stabilities: an LES study, Wind Energy Science 1 (2) (2016) 129–141.

[42] M. Bastankhah, F. Porté-Agel, A new analytical model for wind-turbine wakes, Renewable Energy 70 (2014) 116–123.

[43] I. Katic, J. Hjstrup, N. Jensen, A Simple Model for Cluster Efficiency, A. Raguzzi, 1987, pp. 407–410.

[44] MathWorks, Curve fitting toolbox - matlab, `https://in.mathworks.com/products/curvefitting.html`, (Accessed on 10/21/2019) (2019).

[45] S. H. Shahalami, D. Farsi, Analysis of load frequency control in a restructured multi-area power system with the kalman filter and the LQR controller, AEU - International Journal of Electronics and Communications 86 (2018) 25–46.

[46] MathWorks, https://in.mathworks.com/products/sysid.html?requesteddomain=, `https://in.mathworks.com/products/sysid.html?requestedDomain=`, (Accessed on 10/21/2019) (2019).

[47] K. Thomsen, P. Sørensen, Fatigue loads for wind turbines operating in wakes, Journal of Wind Engineering and Industrial Aerodynamics 80 (1-2) (1999) 121–136.

[48] R. Burra, A. Ambekar, H. Narang, E. Liu, C. Mehendale, L. Thirer, K. Longtin, M. Shah, N. Miller, GE brilliant wind farms, in: 2014 IEEE

Symposium on Power Electronics and Machines for Wind and Water Applications, IEEE, 2014.

Lidar assisted wake redirection in wind farms: A data driven approach

Harsh S. Dhiman[a], Dipankar Deb[a], Aoife M. Foley[b]

[a] *Department of Electrical Engineering, Institute of Infrastructure Technology Research and Management, Ahmedabad, India 380026.*
[b] *School of Mechanical and Aerospace Engineering, Queens University, Belfast, Northern Ireland, United Kingdom BT9 5AH*

Abstract

Lidar based wind measurement is an integral part of wind farm control. The major issues and challenges in power maximization include the potential losses due to wake effect observed among wind turbines. This manuscript presents a wake management technique that utilizes lidar simulations for wake redirection. The proposed methodology is validated for 2-turbine and 15-turbine wind farm layouts involving a PI control based yaw angle correction. Yaw angle misalignment using wake center tracking of the upstream turbines is used to increase the power generation levels. Results of wake center estimation are compared with a Kalman filter based method. Further, the velocity deficit and overall farm power improvement by yaw angle correction is calculated. Results reveal a 1.7% and 0.675% increase in total wind farm power for two different wind speed cases.

Keywords: Center of Wake, Lidar, Transfer function, Velocity deficit, Yaw angle, Wake effect

---

Abbreviations

HAWT Horizontal Axis Wind Turbine

Email addresses: harsh.dhiman.17pe@iitram.ac.in (Harsh S. Dhiman), dipankardeb@iitram.ac.in (Dipankar Deb), a.foley@qub.ac.uk (Aoife M. Foley)

IPC	Individual Pitch Control
LIDAR	Light Detection and Ranging
PI	Proportional Integral Control

1. Introduction

Growing energy demands are rapidly facilitating the wind turbine installations globally in the form of large wind parks to convert the energy available from moving air to electrical energy. Due to constrained land area and cost of equipment one has to design a proper wind farm layout for energy generation [1]. Wind power capture by wind turbine is affected by many factors like wind direction, speed and optimal turbine spacing [2]. For a given terrain, wind turbines must be placed at an optimal operating distance from each other to avoid potential derating caused by wind wakes which are aerodynamic phenomena leading to (a) reduction in wind speed magnitude at the downstream turbine, and (b) increased air turbulence causing mechanical loading on the turbine structure [3]. Sethi et al. presented the modelling of wind farms considering wake interactions [4]. The wake effect is studied in terms of effective wind speed for wind farm layouts. Wind wakes typically are dominant over near wake and far wake region that extend up to $4D_0$ and $8D_0$ respectively, where D_0 is the rotor diameter. Wind wakes causing power loss for an individual wind turbine, has led to the development of many analytical and field models to study the same [5].

Among analytical models, Jensen's [6], Frandsen's [7] and Ainslie's [8] wake model form kinematic wake models, which commonly use algebraic equations to characterize wake deficit. Jensen's wake model is validated and tested for accommodating the power losses due to wake effect and are found in an acceptable range of 10-20% [9, 10, 11, 12]. A new two dimensional Jensen wake model is proposed by Tian et al. that incorporates a variable wake decay rate rather than a constant one. Numerical simulations are performed for computing the wake deficit and are compared with field measurements. Results reveal that such a wake model underestimates for near-wake regions [13]. Ishihara et al. have presented an analytical model that encapsulates the effect of thrust coefficient and air turbulence on the wake deficit [14]. The numerical simulations are compared with a test carried out in wind tunnel and results of the proposed analytical model are in good agreement with experimental analysis. In terms of Large-eddy simulation (LES), the wake flow is studied in neutral atmospheric boundary layer, where the aerodynamic effects on the rotor body and blade element are modeled separately in order to assess power losses [15, 16, 17].

Experimental results from a wind turbine with rotor diameter 0.9 m placed 4 rotor diameters from the wind inlet section and wake velocity distribution, and measured at a downstream distance of $0.6D_0$ and $3D_0$ have shown up to 40% power loss and 80% increased dynamic loading on the turbine structure [18]. Wake study is also important in Wind farm layout optimization (WFLOP) where optimal placement of the wind turbines leads to to minimum wake effect and maximum power capture [19]. Gonzalez et al. have further discussed an evolution based algorithm for optimal wind farm layout [20] to determine net power produced considering the losses occurred due to wake effects. Pitch and yaw angle control techniques are two common ways of increasing power capture. Schlipf et al. demonstrated a Proportional-Integral (PI) control based pitch controller that mitigates dynamic load variations in rotor speed caused due to severe conditions up to 80% [21]. The performance of a traditional feedback control is tested against feed-forward blade pitch control to achieve dynamic load mitigation along with improved life. Results reveal that the feed-forward controller performs better [22].

Vali et al. have utilized a MPAC method for wind farms, to minimize the reference error in wind farm [23]. A methodology based on adjoint MPC is implemented for 6-turbine wind farm where the time-varying signal is tracked against a reference power. Experimental analysis for power improvement using yaw control is studied in [24] for longitudinal distances of $3D_0$ and $6D_0$. In terms of power optimization, a yaw angle based approach is adopted, for single column wind farm layout where axial induction factor for downstream turbines is kept fixed [25]. An experimental study for a small-scale turbine with wake structure and turbine parameters such as yaw angle, pitch angle and tip speed ratio are monitored for a favorable operating performance [26]. In [27], Lidar assisted measurements along with a look-ahead controller is adopted to curb dynamic load through fatigue analysis. A concept of an equivalent load generated given the load is subjected to exact load for its entire lifetime is utilized. In [28], for generator speed regulation, a wind-scheduled control is analysed where for the conditions above rated value, Lidar based control suppresses the irregularities in an accurate wind speed measurement. In [29], Lidar is leveraged to trace the flow caused due wake effect and a desired yaw angle set point is achieved.

In a wind farm where the power losses are incurred due to wake, velocity deficit can be used as a standardized parameter to characterize losses. Given the spatial coordinates (a, b, c) representing the position in the wake field representing maximum power loss, the region is termed as the wake center. Cacciola et al. have used the hub loads and sensors at the downwind turbine to acquire wind velocity deficit data and horizontal shear via an optimization approach for wake center detection without considering yaw misalignment [30]. In [31], authors have discussed an autonomous wake characterization approach to identify wake center position for nonidentical atmospheric conditions. A Doppler lidar is used to scan from January 2017 to June 2017 and results indicate that the wake center position shifts when stable atmospheric conditions exist. Raach et al. explored the possibility of implementing a H_∞ controller for wake redirection based on yaw angle control and a closed-loop performance for the system is analysed [32]. In [33], a wake management strategy is presented using adaptive control technique for wind farms where uncertainties are dominant. Further in [34], decision making and control aspect for a hybrid wind farm are discussed.

The prime contribution of this manuscript is LIDAR based simulation for closed-loop wake center control. The wind turbine and wake are modeled as transfer functions and the estimated wake center is made to follow a desired reference yaw angle trajectory. The proposed methodology is validated for a 15 turbine wind farm layout and the power improvement for each turbine is assessed when upstream turbine(s) are yawed. The wake center estimation are compared with Kalman filter estimations. The subsequent sections are organized as follows. Section 2 entails wake center estimation for multi-model and multiple wake scenario based on proposed transfer function based methodology and Kalman filter. Section 3 highlights performance parameters like farm power production and air turbulence whereas Section 4 discusses the simulation results for proposed methodology and Kalman filter method for a 15-turbine farm configuration. Section 5 highlights discussions, and is followed by Conclusions.

2. Multi-model Wake center estimation and control of Wind Farms

Closed-loop control methodology, as applied to wind farms, primarily built around two main tasks: (i) measures the estimated wind field and, (ii) controls the wake center position. Wind field measurement using lidar accurately processes the controller requirements. LIDAR (Light Detection and Ranging System) sensor utilizes laser based detection and ranging to measure an upstream turbine's effective wind speed at d_{lidar}, the lidar distance. The yaw angle modification potentially reduces the power delivered by an upstream turbine and causes the reverse effect on the downstream turbine. The calculation of the wind speed is done prior to the interaction of the incident wind with the turbine, so as to provide sufficient time for real-time control action [35]. Subsystems related to closed-loop control based on PI control of wake center estimation are described next for desired yaw angle, in Figure 1.

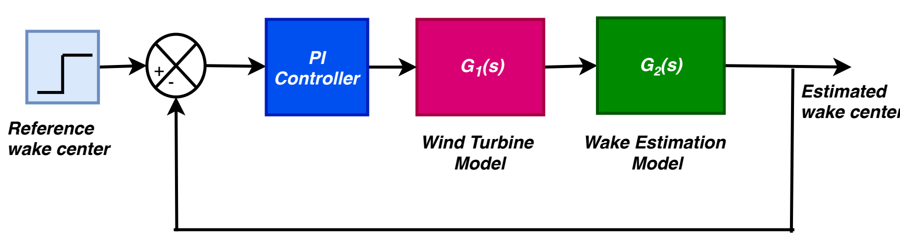

Figure 1: Block diagram for the system under study

2.1. Wind turbine model and wake center estimation

Using actuator disk theory, the power delivered from i^{th} turbine is given as

$$P_i = \frac{1}{2}\rho A_0 C_p u_i^3, \tag{1}$$

for density of air ρ, swept area A_0, power coefficient C_p, and wind speed u_i for i^{th} turbine [36]. However, for wind turbines in yawed condition, the output obtained from an upstream turbine is modified by $\cos^q \gamma$, with q being a tunable parameter in the range $(1.4, 2.2)$ as reported by Fleming et al. [37]. The yaw dynamics for an upstream turbine is expressed as

$$\ddot{\gamma} + 2\zeta\omega\dot{\gamma} = \omega^2\left(\gamma_{ref} - \gamma\right), \tag{2}$$

for undamped eigen frequency ω, damping factor ζ, desired yaw angle γ_{ref}.

The transfer function is estimated with an accuracy of 99.99% using system identification toolbox with γ_{ref} as input and γ as the actual yaw angle, which is varied from (-25°, 25°), with $n_p = 2$ poles and $n_z = 1$ zero, determined as

$$G_1(s) = \frac{0.533s + 0.01094}{s^2 + 0.1538s + 0.002736}. \tag{3}$$

Optimized output in yawed condition of a turbine as formulated by Qian et al. [38] is expressed as

$$P_i = \frac{1}{2}\rho A_0 C_p u_i^3 \cos^2(\gamma_i). \tag{4}$$

The deflection in wake flow caused due to yaw position for a given upstream turbine, as postulated by Jimnez et al. [39], is

$$\delta(d) = \frac{\xi_{init}\left(15\left(\frac{2k_d d}{D_0}+1\right)^4 + \xi_{init}^2\right)}{\frac{30k_d}{D_0}\left(\frac{2k_d d}{D_0}+1\right)^5} - \frac{\xi_{init} D_0 (15 + \xi_{init}^2)}{30k_d}, \tag{5}$$

$$\xi_{init}(\gamma, C_T) = \frac{1}{2}\cos^2(\gamma)\sin(\gamma) C_T, \tag{6}$$

where ξ_{init} is the initial wake angle, d is the scanning or preview distance used by lidar, D_0 is the rotor diameter, k_d is the uncertain model parameter and C_T is the thrust coefficient.

For computation of wake center deflection with changing yaw angles, appropriate lidar distance d_{lidar} is chosen for accurate calculation of the transfer function [40]. A suitable value of the model parameter k_d is selected as 0.15 owing to the turbine operation in neutral boundary layer [41]. The transfer function with 93.76% accuracy for $n_p = 2$ poles and $n_z = 0$ zeros, is of the form

$$G_2(s) = \frac{-0.158}{s^2 + 2.56 \times 10^{-12}s + 0.2404}. \tag{7}$$

The wake center needs to be controlled to ultimately maximize the wind farm power generated. A simple PI controller is tuned using tuning feature of MATLAB/Simulink, is described as

$$f = K_p\Big(\delta(\gamma) + \frac{1}{T_i}\int \delta(\gamma)dt\Big), \tag{8}$$

where $\delta(\gamma)$ is the estimated wake center, K_p, T_i are the proportional gain and time constant.

2.2. Multi-model Wake center control

The accuracy of the estimation of wake center relies on aspects such as ξ_{init}, d, rotor diameter (D_0) and k_d as in (5). Multi-model wake center estimation is studied with constant k_d, and the scanning distance, d_{lidar} is modified in multiples of D_0. Table 1 highlights the estimation accuracies of the transfer function models. Using system identification toolbox and different lidar scanning distances, the best fit models are obtained.

Table 1: Estimation accuracies for different lidar scanning distances

Scanning distance, d_{lidar}	Estimation Accuracy (%)
$1D_0$	93.76
$1.5D_0$	95.08
$2D_0$	94.94
$2.5D_0$	94.82
$3D_0$	94.71

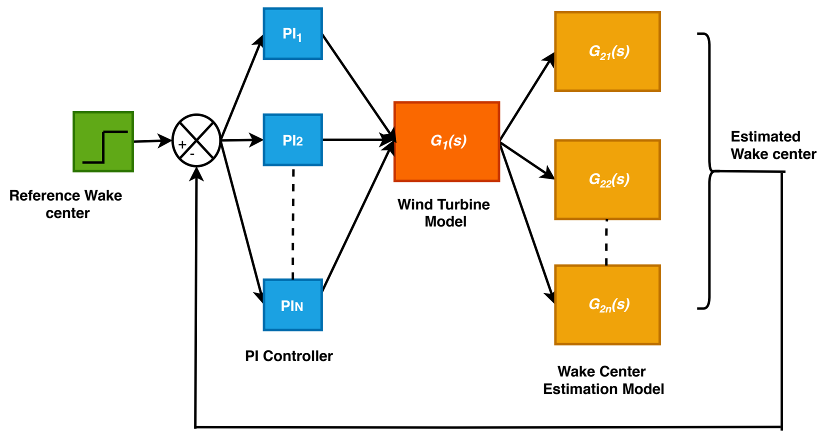

Figure 2: Multi-model wake center estimation

Figure 2 illustrates wake center estimation for a multi-model scenario. Bastankhah and Porte-Agel [42] describe a wake model which follows a Gaussian profile for wind speed deficit. Mathematically, it is expressed as a function of thrust coefficient C_T, radial distance r, and wake width x.

$$v = v_0\Big(1 - A(x)e^{\frac{-r^2}{2\sigma^2}}\Big), \tag{9}$$

$$A(x) = 1 - \sqrt{1 - \frac{C_T}{8(\sigma/D_0)^2}}, \tag{10}$$

$$\frac{\sigma}{D_0} = k\frac{x}{D_0} + \epsilon, \tag{11}$$

where $A(x)$ denotes the maximum normalized velocity deficit for a distance x, and wake width σ which is a function of k representing wake entrainment constant. According to linear superposition principle, the wake deficit due to upstream turbine(s) is expressed as

$$\Delta v_i = \sum_{j=1}^{N}\Big(1 - \frac{v_j}{v_0}\Big), \tag{12}$$

for j^{th} upstream turbine, overall velocity deficit Δu_i at i^{th} downstream turbine, and total upstream turbines N. In [43], a quadratic superposition is presented and is expressed as

$$\Delta v_i = \sqrt{\sum_{j=1}^{N}(\Delta v_j)^2}. \tag{13}$$

In non-yawed conditions, power generated at the downstream turbine dwindles because of shadow effect of upstream turbines, and requires effective wake management. Yawing the upstream turbine effectively controls the wake center, and to account for multiple wakes on a downstream turbine from a multiple of upstream turbines, the transformed thrust coefficient $C_T \cos^3(\gamma_{w,j})$, where $\gamma_{w,j}$ denotes the yaw angle for the j^{th} upwind turbine. Further, modified velocity deficit for i^{th} downstream turbine is expressed as

$$v_i = v_0\Big(1 - A_{ij}(x)e^{\frac{-r^2}{2\sigma_{ij}^2}}\Big), \tag{14}$$

$$A_{ij}(x) = 1 - \sqrt{1 - \frac{C_T \cos^3(\gamma_{w,j})}{8(\sigma_{ij}/D_0)^2}}, \tag{15}$$

$$\frac{\sigma_{ij}}{D_0} = k\frac{x_{ij}}{D_0} + \epsilon, \tag{16}$$

$$\beta_w = 0.5\left(\frac{1+\sqrt{1-C_T}}{\sqrt{1-C_T}}\right), \tag{17}$$

where $\epsilon = 0.25\sqrt{\beta_w}$, σ_{ij} represents wake width at downstream distance x_{ij} between j^{th} upstream and i^{th} downstream turbine. The velocity deficit for each upstream turbine is computed using (14) for yaw angle $\gamma_{w,j}$ and for N upstream turbines, the overall velocity deficit at i^{th} downstream turbine is calculated based on the principle of quadratic superposition in (13). Figure 3 illustrates the proposed methodology for wake redirection for multiple upstream turbines.

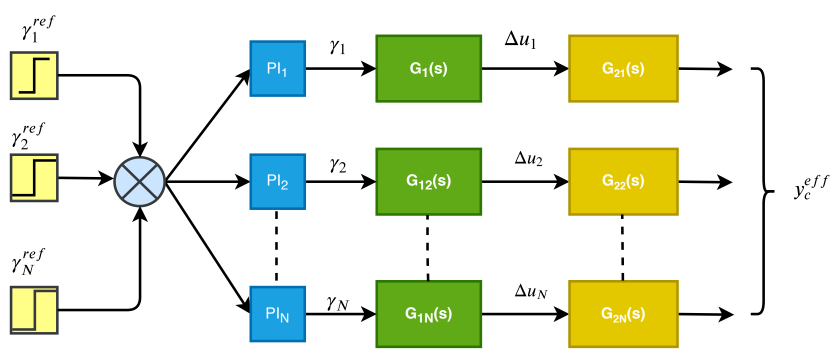

Figure 3: Multiple wake scenario based wake center estimation

Transfer function models with Multiple-Input Single Output (MISO) configuration are evaluated for best estimation accuracy, and is expressed as

$$g(y_c) = v_m e^{\frac{-(y_c-\mu_y)^2}{2\sigma_{lidar}^2}}, \quad (18)$$

$$\sigma_{lidar} = k d_{lidar} + \epsilon D_0, \quad (19)$$

where y_c, μ_y represent the height of hub and position of the wake center respectively given an overall velocity deficit of $g(y_c)$ for a lidar scanning distance d_{lidar} and v_m denotes the maximum velocity deficit. The empirical relationship between effective velocity deficit and effective wake center is estimated using curve fitting toolbox in MATLAB [44]. In the curve fitting toolbox, the input quantity is considered as velocity deficit and output quantity as effective wake center deflection. Using these quantities the curve fitting toolbox utilized for appropriate fitting.

Developed in 1960, Kalman filter is being actively used to estimate the states in the noisy or disturbed environments. State estimation as perceived by a Kalman filter is based on a recursive process of a noisy data [45], and is expressed mathematically as

$$\hat{x}_{t+1} = \mathbf{A}x_t + \mathbf{B}u_t + w_t, \quad (20)$$

$$\hat{y}_t = \mathbf{C}x_t + \mathbf{D}u_t + v_t, \quad (21)$$

where $\mathbf{A}, \mathbf{B}, \mathbf{C}, \mathbf{D}$ represent the state-space matrices of the plant, w_t, v_t are process and measurement noise at time step t respectively and $\hat{x}_{t+1}$ is the updated state vector at time step $t + 1$. For the current scenario, Kalman filter technique is implemented to derive an estimate of the wake center trajectory for a set of upwind and downwind turbines. Using system identification toolbox, the transfer function models are computed with yaw angle as input and wake center deflection as output. In Figure 4, a schematic representation for Kalman filter based wake center is illustrated.

The state-space model can be estimated using system identification toolbox available in MATLAB [46]. In this toolbox, the input and output data are fed with a 'double' variable which represents a time-varying quantity. The model simulations can be run for different system orders in order to obtain maximum

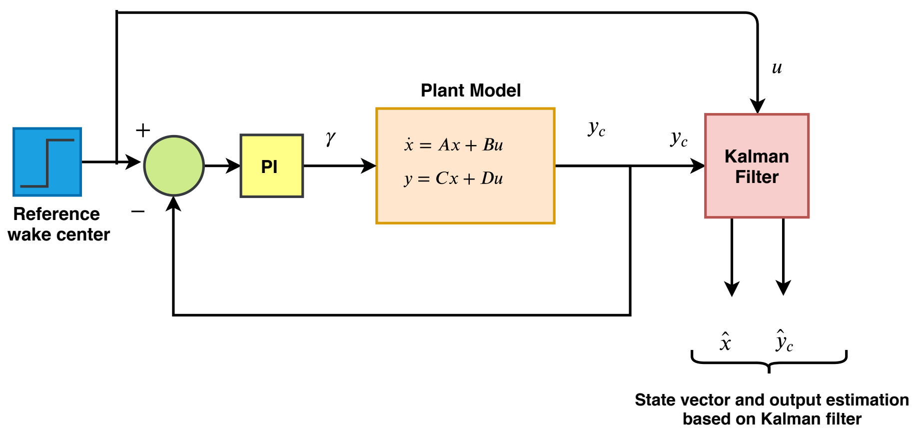

Figure 4: Kalman filter technique based wake center estimation

estimation accuracy. From here, the state-space model can be exported and can be used according to the user need.

3. Performance parameters for waked wind farms

Power maximization and optimization of the land available are the two prime objectives for wind farm operators. In case of wake effect, the reduction in power capture is compensated by either changing yaw alignment or changing lateral position of downstream turbine. Since micro-siting is done in priori, yaw misalignment is the preferred choice. Power capture and air turbulence are the two main parameters that affect the performance of a wind farm. Jensen's wake model computes wind speed at distance h and a distance r radially from the wake center line is expressed as

$$v(h,r) = v_0\Big[1 - 2a\Big(\frac{r_0}{r_0 + kh}\Big)^2\Big], \tag{22}$$

where v_0 is the freestream wind velocity, r_0 denotes rotor radius and k represents wake entrainment factor. The flow behind upwind turbine is deflected by Ω_j when yaw angle is aligned at $\gamma_{w,j}$ and wind direction θ_j expressed as

$$\Omega_j = (0.6a_j + 1)\gamma_{w,j} + \theta_j, \tag{23}$$

where a_j is the axial induction factor for turbine $j \in H$ (upstream turbines). Velocity profile for a downwind turbine with yaw misalignment is given as

$$v_i(x,r) = \begin{cases} v_0\Big[1 - 2a_j\Big(\dfrac{1}{1+2kT\cos(\Omega_j)}\Big)^2 \times \cos^2(4.5\Omega_j)\Big], & \Omega_j \leq 20^\circ \\ v_0, & \Omega_j > 20^\circ, \end{cases} \tag{24}$$

where $T = \frac{h}{D_0} \in [2, \ldots, 5]$ denotes the spacing factor which is a multiple of rotor diameter. A yaw angle of $\gamma_{w,j}$ on the upstream turbine WT_j diverts the wake flow for a downwind turbine WT_i by an angle of Ω_j arrives at a velocity profile like (24). A yawed upstream turbine now captures power which is changed by a factor of $\cos^3 \gamma_w$.

Further, dynamic loading on downstream is a challenging issue that causes catastrophic damage to rotor blades and tower. The resulting air turbulence can be reduced by changing yaw angle $\gamma_{w,j}$ of upstream turbine. Mathematically, the overall turbulence intensity is given as

$$E_{eff} = \sqrt{E_a^2 + K^2 \sum_{j=1}^{N} (1 - \sqrt{1 - C_T \cos\gamma_{w,j}}) h_i^{-2/3}}, \tag{25}$$

where E_a denotes the ambient air turbulence whereas E_{eff} being computed for a downwind distance h_i for N upstream turbines and K is constant with a value of 0.93 [47].

4. Numerical Simulations for Proposed Methodology

Next, the proposed methodology for closed-loop control of wake center for 2-turbine and 15-turbine wind farm layout is presented. For 2-turbine wind farm, the intent is to track wake center of WT_1 (upwind) and examine the impact on the performance parameters of WT_2 (downstream).

Throughout the simulation, wind turbines with same rotor diameter of 80 meters are considered. WT_1 and WT_2 are placed 400 meters apart. The wake center is estimated using lidar simulation for desired yaw control based on methodology discussed in Section 2. Initially, the yaw angle of WT_1 is $\gamma_w = 0^\circ$

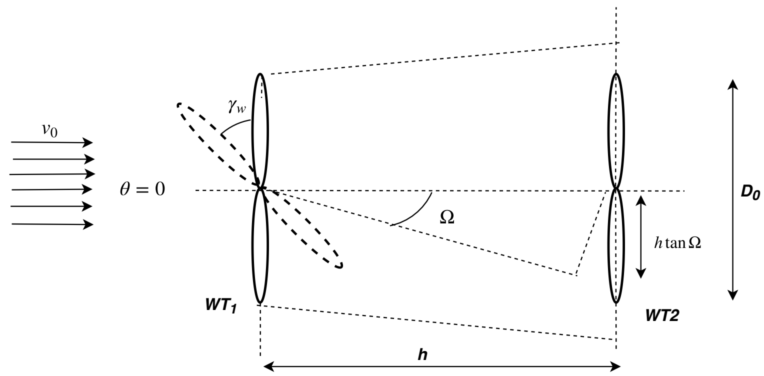

Figure 5: 2-turbine layout for wake deflection

and lidar scanning distance is kept $1D_0$. In order to validate the proposed methodology, a 500 second simulation is carried out for 2-turbine layout. Figure 6 illustrates the wake center simulation using proposed methodology.

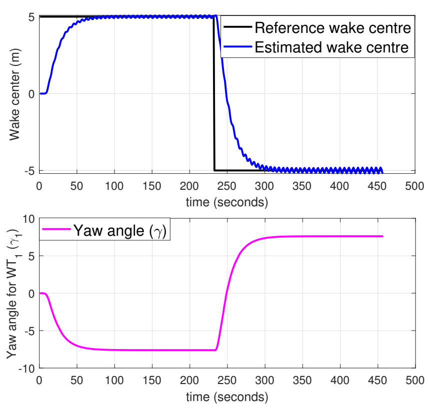

Figure 6: Desired yaw angle alignment and wake center for 2-turbine layout

The wake center reference is changed at t=250 seconds for desired yaw angle setting based on a PI control technique. Based on this, a 1000 second simulation is carried out to evaluate the performance parameters for 2-turbine wind farm layout. The yaw angle setting for WT_1, γ_w is changed at t=500 second where the mean wind speed is changed from 8 m/sec to 10 m/sec.

From Figure 7, it is observed that the total wind power extracted has increased by 7.52%. In a similar study presented by Raach et al. [29] with same rotor diameter of turbines, the total power increase is reported around 4.5%.

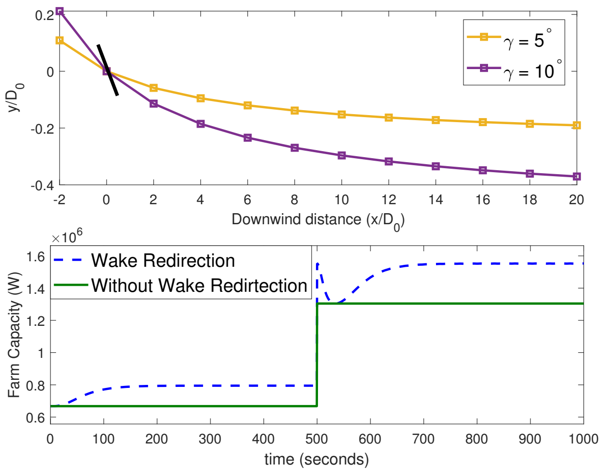

Figure 7: Wake deflection and power output with and without redirection

The net wind farm power increases due to high fidelity lidar measurements that accurately measure the deflection caused by yaw misalignment. The yaw angle misalignment also affects the air turbulence intensity on downstream wind turbine. For a fixed yaw angle of an upstream turbine, the turbulence decreases as the longitudinal distance between the turbines is increased. Figure 8 illustrates the turbulence acting on WT_2 as a result of varying downstream distance.

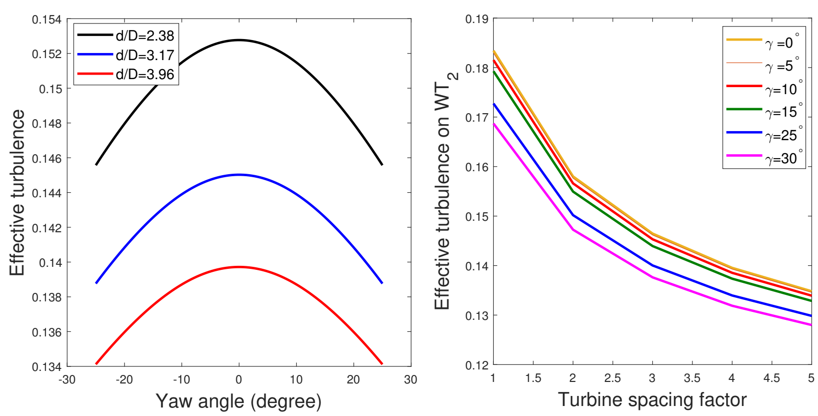

Figure 8: Effective air turbulence at WT_2

Keeping longitudinal distance fixed, for given yaw misalignment, the effective turbulence acting on WT_2 is found minimum for $\gamma_w = 30°$. Wake center control is analyzed for a 15 turbine wind farm with WT_{12} facing wake effect from $WT_2, WT_3, WT_4, WT_5, WT_7, WT_9$ and WT_{10}. In Figure 9, the distances between turbines in terms of rotor diameter are illustrated. Yaw angles of upstream turbines WT_j for $j \in [2, 3, 4, 5, 7, 9, 10]$ are chosen as $\gamma_2 = 2°$, $\gamma_3 = 2.5°$, $\gamma_4 = 5°$, $\gamma_5 = 7°$, $\gamma_7 = 9°$, $\gamma_9 = 10°$ and $\gamma_{10} = 15°$ and when yawed, the wake center deflection is controlled by determining effective velocity deficit.

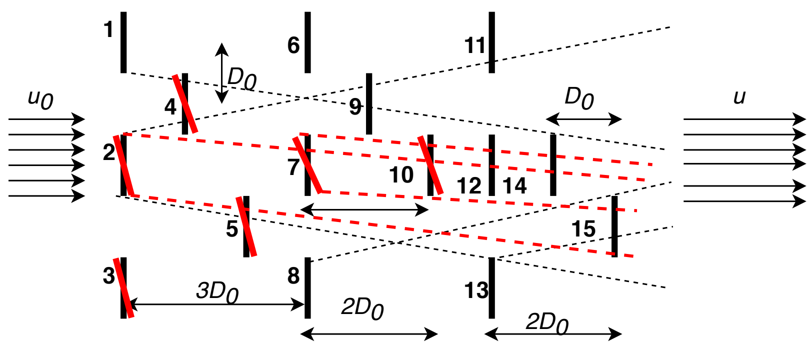

Figure 9: 15 turbine layout in non-yawed (black solid line) and yawed mode(red solid line)

The empirical relationship between overall velocity deficit and wake center deflection (18) is converted into an overall transfer function having multiple-inputs and single output (MISO) topology. LIDAR is mounted at nacelle of WT_{12} that scans the wind flow for all upwind turbines. For estimating the wake width, a scan distance $d_{lidar} = 2D_0$ is considered.

In Figures 10 and 11, the wake center estimation by the proposed transfer function methodology and by Kalman filter based technique is presented.

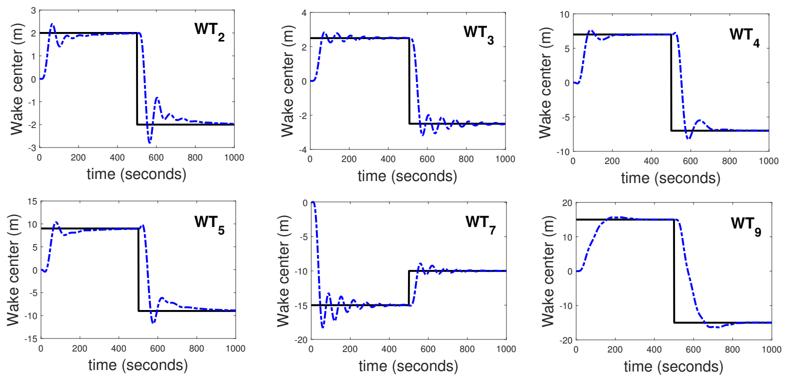

Figure 10: Wake center estimation by proposed model (blue dotted line) and reference wake center (black solid line) for upwind turbines of WT_{12}

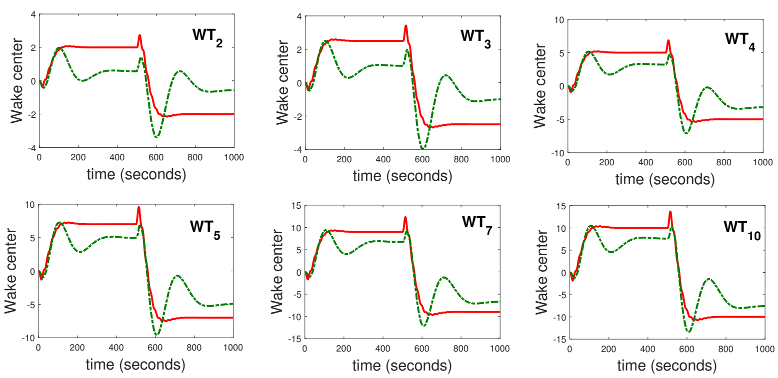

Figure 11: Wake center estimation by proposed model (red solid line) and Kalman filter (green dotted line) for upwind turbines of WT_{12}

5. Discussions

The wind turbine power improvement in the 15-turbine farm layout when operated in yaw mode is tested for a wind profile of 500 seconds illustrated in Figure 12.

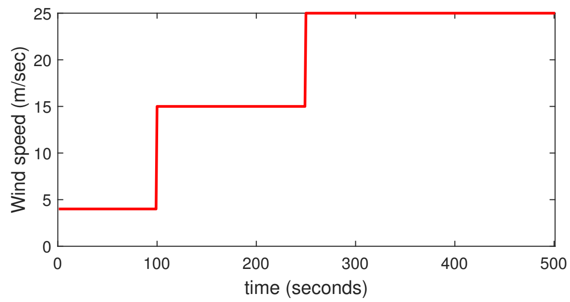

Figure 12: Wind speed profile for the range 4-25 m/sec

The wind in this case ranges from 4 m/sec to 25 m/sec. For the first 100 seconds the wind speed us 4 m/sec, the from 100 to 250 seconds wind speed is 15 m/sec and for the last 250 seconds the speed is 25 m/sec. The mean wind power captured by each wind turbine is calculated for non-yawed (P_{ny}) and yawed (P_y) scenario. Table 2 depicts the improvement in wind power captured for each turbine and it is observed that for WT_1 the wind power captured remains same as it is not yawed. For WT_2 and WT_3, the wind power decreases in yawed mode as they are the upstream turbines. For turbines WT_4 to WT_{15}, the power captured in yawed mode increases as yawing deflects the wake away from downstream turbine. Overall, for the wind speed profile illustrated in Figure 12, the mean power captured by the wind farm in non-yawed mode is 160.3364 MW while in yawed mode it is 161.418 MW thus indicating an increase of 0.675%.

Table 2: Mean turbine power in non-yawed and yawed condition for wind profile in the range 4-25 m/sec

Turbine	Upwind Turbine	Power (P_{ny}) (MW)	Power (P_y) (MW)	% change
WT_1	NA	14.3044	14.3044	0.00
WT_2	NA	14.3044	14.2782	-0.183
WT_3	NA	14.3044	14.2636	-0.285
WT_4	1,2	10.9830	10.9890	+0.0546
WT_5	2,3	11.704	11.709	+0.0427
WT_6	1,4	12.215	12.219	+0.0327
WT_7	2,4,5	9.4873	9.4918	+0.047
WT_8	3,5	10.0182	10.188	+1.690
WT_9	1,4,6,7	9.2660	9.2704	+0.0475
WT_{10}	2,5,7,9	9.2478	9.2519	+0.0440
WT_{11}	1,2,4,6,9	8.9314	9.09320	+1.811
WT_{12}	2,3,4,5,7,9,10	8.9126	9.09261	+1.2734
WT_{13}	3,5,8	8.8956	9.0942	+2.2320
WT_{14}	2,3,4,5,7,9,10,12	8.8831	9.0988	+2.3130
WT_{15}	2,5,7,8,10,12,13,14	8.8792	9.0987	+2.3511
		$\sum P_{ny} = 160.3364$	$\sum P_y = 161.418$	

Table 3: Wind turbine power captured for non-yawed and yawed scenario with wind speed range 8-10 m/sec

Turbine	Upwind Turbine	Power (P_{ny}) (MW)	Power (P_y) (MW)	% change
WT_1	NA	2.8274	2.8274	0.00
WT_2	NA	2.8274	2.8223	-0.1800
WT_3	NA	2.8274	2.8223	-0.1800
WT_4	1,2	1.5074	1.5116	+0.2786
WT_5	2,3	2.6816	2.6916	+0.3729
WT_6	1,4	2.0666	2.0891	+1.0887
WT_7	2,4,5	2.0561	2.1541	+4.7663
WT_8	3,5	2.0162	2.1130	+4.8011
WT_9	1,4,6,7	2.0053	2.1016	+4.8022
WT_{10}	2,5,7,9	2.0001	2.0884	+4.4414
WT_{11}	1,2,4,6,9	2.0761	2.0962	+0.9681
WT_{12}	2,3,4,5,7,9,10	1.9821	1.9959	+0.6962
WT_{13}	3,5,8	2.0752	2.0965	+0.9782
WT_{14}	2,3,4,5,7,9,10,12	1.9701	1.9862	+0.8172
WT_{15}	2,5,7,8,10,12,13,14	1.9970	2.0866	+4.4867
		$\sum P_{ny} = 32.916$	$\sum P_y = 33.483$	

Results from Figures 10 and 11 indicate that Kalman filter based technique fails to track the wake center deflection accurately due to nonlinear nature and stochastic of wind speed. Contrary to Kalman filter, the proposed transfer function based technique tracks the reference wake center with accuracy. The velocity deficit caused due to each upwind turbine for this layout is computed both in yawed and non-yawed conditions using the Gaussian wake profile (13). In Figure 13, the overall velocity deficit in yawed mode the deficit is 6.15% less than that in non-yawed mode.

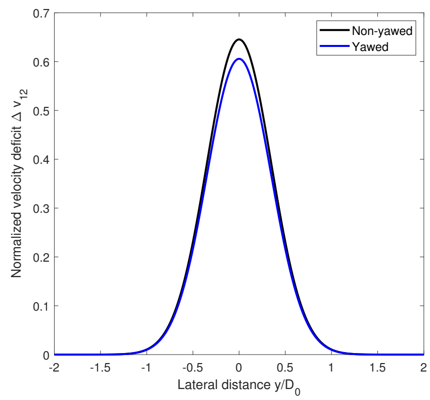

Figure 13: Non-yawed and yawed scenarios for overall velocity deficit

Further, Figure 14 illustrates the normalized velocity at WT_{12} for different upwind turbines.

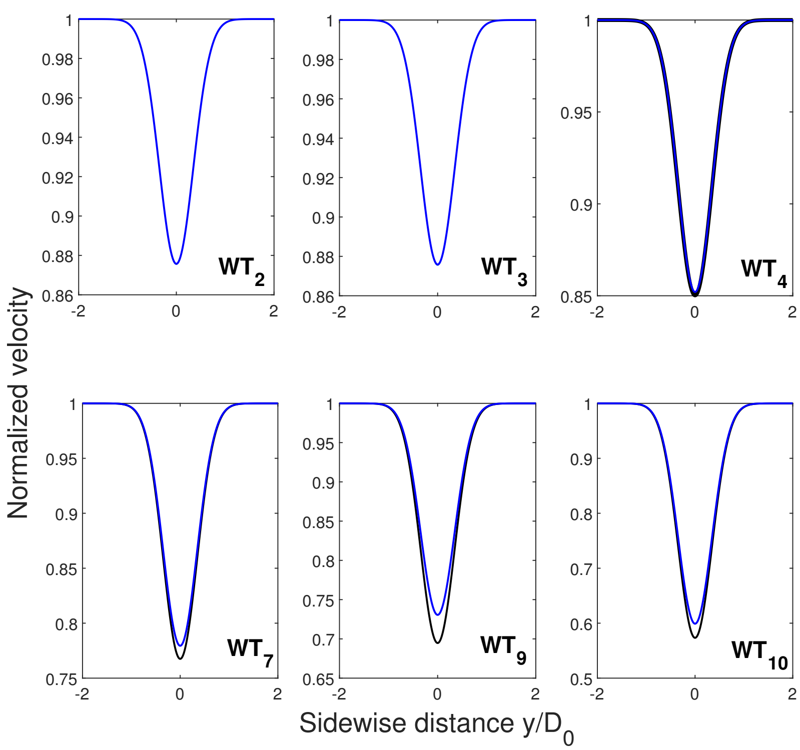

Figure 14: Normalized velocity for WT_{12} for non-yawed (black) and yawed (blue) scenario

Velocity for WT_2 and WT_3 renders the fact that the due to the large longitudinal distance ($6D_0$) to WT_{12}, the velocity deficit with yaw misaligned is not pronounced. Further, for WT_7, WT_9 and WT_{10} power capture is found to be notable when the upwind turbines are yawed. At $y/D_0 = 0$, the turbine power is minimum as it indicates the wake center position. Table 3 highlights the wind power tapped by respective turbines with reference to the layout shown in Figure 9. The powers for non-yawed (P_{ny}) and yawed (P_y) scenario are calculated with a freestream wind speed of $v_0 = 10$ m/sec, and the power capture with yawed upwind turbines outperforms that in non-yawed scenario for each turbine. A 1.7% rise in the overall farm power is observed with operation in the yawed scenario. In other related analyses for power maximization with yaw correction, Adaramola et al. carried a wind tunnel experiment to study the outcome of yawing the upwind turbine on the downwind turbine [24] and observed a noteworthy increase in the power coefficient of downstream turbine at $3D_0$ downstream distance away. Since the proposed methodology is solely based on the transfer function blocks, the computational complexity for analyzing the wind farm performance does not arise. Dynamic scenarios in the atmospheric boundary layer pose significant challenges to wake center estimation in form of turbulent eddies that arise due to Coriolis forces. With availability of accurate wind measurement devices like Lidar, wind farm controllers can take appropriate actions to cope with time periods of power sags. Further, experimental investigation carried out by General Electric suggests that managing turbulent wakes increases the plant energy output in the range of 0.5-2% [48].

6. Conclusions and Future scope

A novel closed loop control methodology aimed at effective tracking of the wake center of the upwind turbine, that is based on transfer function formulation is proposed in the present work. Taking leverage of a data drive approach, a transfer function model relating yaw angle and wake center for a multiple wake case is estimated. To determine the effective wake center for a given upwind turbine WT_{12}, the overall velocity deficit as seen by WT_{12} is used. Utilizing advanced controllers, wake management integrates scenarios that deal with stochastic wind environment along with micro-siting related issues. In the present case, lidar based measurement methodology outperforms Kalman filter technique in a more accurate wake center estimation. Scenarios with different wind conditions in the range of 8-10 m/sec and 4-25 m/sec are tested and results indicate an increase of 1.7% and 0.675% respectively. This study can be extended in future for offshore wind platform where the dominant wave-current will have a significant influence on the dynamic loading of the turbine structure.

Acknowledgements

Dr Foley's research is funded by the Northern Ireland Department for Economics, the Engineering and Physical Sciences Research Council (EPSRC) and NSFC jointly funded iGIVE project (EP/L001063/1), the Collaborative REsearch of Decentralization, ElectrificatioN, Communications and Economics (CREDENCE) project, which is funded by a US-Ireland Department for the Economy (DfE), Science Foundation Ireland (SFI), National Science Foundation (NSF) and Research and Development Partnership Program (Centre to Centre) award (grant number USI 110) and the SPIRE2 (Storage Platform for the Integration of Renewable Energy 2) project, funded by the Special European Programmes Body (SEUPB) under the European Unions INTERREG VA programme.

References

[1] S. Chowdhury, J. Zhang, A. Messac, L. Castillo, Unrestricted wind farm layout optimization (UWFLO): Investigating key factors influencing the maximum power generation, Renewable Energy 38 (1) (2012) 16–30.

[2] J. F. Manwell, Wind energy explained : theory, design and application, Wiley, Chichester, U.K, 2009.

[3] C. L. Archer, A. Vasel-Be-Hagh, C. Yan, S. Wu, Y. Pan, J. F. Brodie, A. E. Maguire, Review and evaluation of wake loss models for wind energy applications, Applied Energy 226 (2018) 1187–1207.

[4] J. K. Sethi, D. Deb, M. Malakar, Modeling of a wind turbine farm in presence of wake interactions, in: 2011 International Conference on Energy, Automation and Signal, IEEE, 2011.

[5] T. Göçmen, P. van der Laan, P.-E. Réthoré, A. P. Diaz, G. C. Larsen, S. Ott, Wind turbine wake models developed at the technical university of denmark: A review, Renewable and Sustainable Energy Reviews 60 (2016) 752–769.

[6] N. Jensen, A note on wind generator interaction, 1983.

[7] S. Frandsen, R. Barthelmie, S. Pryor, O. Rathmann, S. Larsen, J. Højstrup, M. Thøgersen, Analytical modelling of wind speed deficit in large offshore wind farms, Wind Energy 9 (1-2) (2006) 39–53.

[8] J. Ainslie, Calculating the flowfield in the wake of wind turbines, Journal of Wind Engineering and Industrial Aerodynamics 27 (1-3) (1988) 213–224.

[9] A. Crespo, J. Hernndez, S. Frandsen, Survey of modelling methods for wind turbine wakes and wind farms, Wind Energy 2 (1) (1999) 1–24.

[10] R. J. Barthelmie, K. Hansen, S. T. Frandsen, O. Rathmann, J. G. Schepers, W. Schlez, J. Phillips, K. Rados, A. Zervos, E. S. Politis, P. K. Chaviaropoulos, Modelling and measuring flow and wind turbine wakes in large wind farms offshore, Wind Energy 12 (5) (2009) 431–444.

[11] F. Porté-Agel, Y.-T. Wu, C.-H. Chen, A numerical study of the effects of wind direction on turbine wakes and power losses in a large wind farm, Energies 6 (10) (2013) 5297–5313.

[12] Y.-K. Wu, Y.-S. Su, Z. Lee, T.-Y. Wu, Estimation of wake losses in an offshore wind farm by WAsP - a real project case study in taiwan, in: 10th

International Conference on Advances in Power System Control, Operation & Management (APSCOM 2015), Institution of Engineering and Technology, 2015. doi:10.1049/ic.2015.0264.

[13] L. Tian, W. Zhu, W. Shen, N. Zhao, Z. Shen, Development and validation of a new two-dimensional wake model for wind turbine wakes, Journal of Wind Engineering and Industrial Aerodynamics 137 (2015) 90–99.

[14] T. Ishihara, G.-W. Qian, A new gaussian-based analytical wake model for wind turbines considering ambient turbulence intensities and thrust coefficient effects, Journal of Wind Engineering and Industrial Aerodynamics 177 (2018) 275–292.

[15] R. J. Stevens, L. A. Martínez-Tossas, C. Meneveau, Comparison of wind farm large eddy simulations using actuator disk and actuator line models with wind tunnel experiments, Renewable Energy 116 (2018) 470–478.

[16] F. Porté-Agel, Y.-T. Wu, H. Lu, R. J. Conzemius, Large-eddy simulation of atmospheric boundary layer flow through wind turbines and wind farms, Journal of Wind Engineering and Industrial Aerodynamics 99 (4) (2011) 154–168.

[17] Y.-T. Wu, F. Porté-Agel, Modeling turbine wakes and power losses within a wind farm using LES: An application to the horns rev offshore wind farm, Renewable Energy 75 (2015) 945–955.

[18] H. Schümann, F. Pierella, L. Sætran, Experimental investigation of wind turbine wakes in the wind tunnel, Energy Procedia 35 (2013) 285–296.

[19] J. Park, K. H. Law, Layout optimization for maximizing wind farm power production using sequential convex programming, Applied Energy 151 (2015) 320–334.

[20] J. S. González, A. G. G. Rodriguez, J. C. Mora, J. R. Santos, M. B. Payan, Optimization of wind farm turbines layout using an evolutive algorithm, Renewable Energy 35 (8) (2010) 1671–1681.

[21] D. Schlipf, M. Kühn, Prospects of a collective pitch control by means of predictive disturbance compensation assisted by wind speed measurements, Proceedings of the 9th German Wind Energy Conference DEWEK, 26th to 27th November, Bremen, Germany, 2008.

[22] F. Dunne, L. Pao, A. Wright, B. Jonkman, N. Kelley, Combining standard feedback controllers with feedforward blade pitch control for load mitigation in wind turbines, in: 48th AIAA Aerospace Sciences Meeting Including the New Horizons Forum and Aerospace Exposition, American Institute of Aeronautics and Astronautics, 2010.

[23] M. Vali, V. Petrovic, S. Boersma, J.-W. van Wingerden, L. Y. Pao, M. Kuhn, Model predictive active power control of waked wind farms, in: 2018 Annual American Control Conference (ACC), IEEE, 2018.

[24] M. Adaramola, P.-Å. Krogstad, Experimental investigation of wake effects on wind turbine performance, Renewable Energy 36 (8) (2011) 2078–2086.

[25] Z. Dar, K. Kar, O. Sahni, J. H. Chow, Windfarm power optimization using yaw angle control, IEEE Transactions on Sustainable Energy 8 (1) (2017) 104–116.

[26] B. Dou, M. Guala, L. Lei, P. Zeng, Experimental investigation of the performance and wake effect of a small-scale wind turbine in a wind tunnel, Energy 166 (2019) 819–833.

[27] D. Schlipf, T. Fischer, C. E. Carcangiu, M. Rossetti, E. Bossanyi, Load analysis of look-ahead collective pitch control using lidar, Proceedings of the 10th German Wind Energy Conference DEWEK, 2010.

[28] V. Rezaei, LIDAR-based robust wind-scheduled control of wind turbines, in: 2014 American Control Conference, IEEE, 2014.

[29] S. Raach, D. Schlipf, P. W. Cheng, Lidar-based wake tracking for closed-loop wind farm control, Journal of Physics: Conference Series 753 (2016) 052009.

[30] S. Cacciola, M. Bertelè, J. Schreiber, C. Bottasso, Wake center position tracking using downstream wind turbine hub loads, Journal of Physics: Conference Series 753 (2016) 032036.

[31] R. J. Barthelmie, S. C. Pryor, Automated wind turbine wake characterization in complex terrain, Atmospheric Measurement Techniques Discussions (2019) 1–31.

[32] S. Raach, D. Schlipf, F. Borisade, P. W. Cheng, Wake redirecting using feedback control to improve the power output of wind farms, in: 2016 American Control Conference (ACC), IEEE, 2016.

[33] H. S. Dhiman, D. Deb, V. Muresan, V. E. Balas, Wake management in wind farms: An adaptive control approach, Energies 12 (7). doi:10.3390/en12071247.

[34] H. S. Dhiman, D. Deb, Decision and Control in Hybrid Wind Farms, Springer Singapore, 2020. doi:10.1007/978-981-15-0275-0.

[35] E. Simley, L. Pao, R. Frehlich, B. Jonkman, N. Kelley, Analysis of wind speed measurements using continuous wave LIDAR for wind turbine control, in: 49th AIAA Aerospace Sciences Meeting including the New Horizons Forum and Aerospace Exposition, American Institute of Aeronautics and Astronautics, 2011.

[36] The wind and wind turbines, in: Wind Turbine Control Systems, Springer London, 2007, pp. 7–28.

[37] P. Fleming, J. Annoni, J. J. Shah, L. Wang, S. Ananthan, Z. Zhang, K. Hutchings, P. Wang, W. Chen, L. Chen, Field test of wake steering at an offshore wind farm, Wind Energy Science 2 (1) (2017) 229–239.

[38] G.-W. Qian, T. Ishihara, A new analytical wake model for yawed wind turbines, Energies 11 (3) (2018) 665.

[39] Á. Jiménez, A. Crespo, E. Migoya, Application of a LES technique to characterize the wake deflection of a wind turbine in yaw, Wind Energy 13 (6) (2009) 559–572.

[40] E. Machefaux, G. C. Larsen, N. Troldborg, M. Gaunaa, A. Rettenmeier, Empirical modeling of single-wake advection and expansion using full-scale pulsed lidar-based measurements, Wind Energy 18 (12) (2014) 2085–2103.

[41] L. Vollmer, G. Steinfeld, D. Heinemann, M. Kühn, Estimating the wake deflection downstream of a wind turbine in different atmospheric stabilities: an LES study, Wind Energy Science 1 (2) (2016) 129–141.

[42] M. Bastankhah, F. Porté-Agel, A new analytical model for wind-turbine wakes, Renewable Energy 70 (2014) 116–123.

[43] I. Katic, J. Hjstrup, N. Jensen, A Simple Model for Cluster Efficiency, A. Raguzzi, 1987, pp. 407–410.

[44] MathWorks, Curve fitting toolbox - matlab, `https://in.mathworks.com/products/curvefitting.html`, (Accessed on 10/21/2019) (2019).

[45] S. H. Shahalami, D. Farsi, Analysis of load frequency control in a restructured multi-area power system with the kalman filter and the LQR controller, AEU - International Journal of Electronics and Communications 86 (2018) 25–46.

[46] MathWorks, https://in.mathworks.com/products/sysid.html?requesteddomain=, `https://in.mathworks.com/products/sysid.html?requestedDomain=`, (Accessed on 10/21/2019) (2019).

[47] K. Thomsen, P. Sørensen, Fatigue loads for wind turbines operating in wakes, Journal of Wind Engineering and Industrial Aerodynamics 80 (1-2) (1999) 121–136.

[48] R. Burra, A. Ambekar, H. Narang, E. Liu, C. Mehendale, L. Thirer, K. Longtin, M. Shah, N. Miller, GE brilliant wind farms, in: 2014 IEEE

Symposium on Power Electronics and Machines for Wind and Water Applications, IEEE, 2014.

LaTeX Source Files
Click here to download LaTeX Source Files: LaTeX_Sourcefiles.zip

***Declaration of Interest Statement**

DECLARATION OF INTEREST

The authors of this manuscript titled **"Lidar assisted wake redirection in wind farms: A data driven approach"** hereby confirm that there is no conflicting interest and the work pertaining to this manuscript is original.

Harsh S. Dhiman

Dipankar Deb

Aoife M. Foley